VTRC
Virginia Transportation Research Council

We Bring Innovation to Transportation

Performance Characteristics of In-Service Bridges for Enhancing Load Ratings: Leveraging Refined Analysis Methods

http://www.virginiadot.org/vtrc/main/online_reports/pdf/21-r20.pdf

DEVIN K. HARRIS, Ph.D.
Associate Professor
Department of Engineering Systems and Environment
University of Virginia

OSMAN OZBULUT, Ph.D.
Associate Professor
Department of Engineering Systems and Environment
University of Virginia

ABDOU K. NDONG
Graduate Research Assistant
Department of Engineering Systems and Environment
University of Virginia

MUHAMMAD SHERIF
Assistant Professor
Department of Civil, Construction and Environmental Engineering
University of Alabama at Birmingham

Final Report VTRC 21-R20

VIRGINIA TRANSPORTATION RESEARCH COUNCIL
530 Edgemont Road, Charlottesville, VA 22903-2454
vtrc.virginiadot.org

Standard Title Page - Report on Federally Funded Project

1. Report No.: FHWA/VTRC 21-R20	2. Government Accession No.:	3. Recipient's Catalog No.:
4. Title and Subtitle: Performance Characteristics of In-Service Bridges for Enhancing Load Ratings: Leveraging Refined Analysis Methods		5. Report Date: March 2021 6. Performing Organization Code:
7. Author(s): Devin K. Harris, Ph.D., Osman Ozbulut, Ph.D., Abdou K. Ndong, and Muhammad Sherif		8. Performing Organization Report No.: VTRC 21-R20
9. Performing Organization and Address: Virginia Transportation Research Council 530 Edgemont Road Charlottesville, VA 22903		10. Work Unit No. (TRAIS): 11. Contract or Grant No.: 114318
12. Sponsoring Agencies' Name and Address: Virginia Department of Transportation 1401 E. Broad Street Richmond, VA 23219 Federal Highway Administration 400 North 8th Street, Room 750 Richmond, VA 23219-4825		13. Type of Report and Period Covered: Final Contract 14. Sponsoring Agency Code:
15. Supplementary Notes: This is an SPR-B report.		

16. Abstract:

Bridge load rating assesses the safe live load carrying capacity of an existing or newly designed structure. In addition to load rating with previously defined standard load rating vehicles, the Federal Highway Administration issued additional guidance to states related to rating requirements for all the bridges with respect to specialized hauling vehicles and emergency vehicles that must be met by the end of 2022. It is recognized that the load effects (bending moment and shear) produced by these vehicle types on certain bridge types and spans might be greater than those caused by the previous rating vehicles. Therefore, a number of bridges within VDOT's inventory may require posting when rated with these specialized vehicles.

The goal of this study was to assess the likelihood of an increase in load rating factors through refined analysis methods for the bridge classes potentially vulnerable to load ratings under consideration of the new federal regulations and when using conventional, simplified equations for load distribution factors. In particular, the study focused on the evaluation of live load distribution factors for girder bridges and effective widths for distributing live loads in slab bridges through refined analysis. Three bridge classes (simple span steel girder bridges, reinforced concrete T-beam bridges, and concrete slab bridges) were selected for this refined analysis. Girder bridges were modeled using the plate-with-an-eccentric-beam analysis approach, while plate elements were used to model slab bridges within the LARSA 4D software package. The selected modeling approaches were validated through the simulation of the bridge structures with available field-testing results from the literature. A total of 71 in-service bridges belonging to the three selected bridge classes were then modeled and analyzed to compute the load distribution factors for girder bridges or effective widths for slab bridges, and the results were compared with those obtained from the code-specified equations. Using the data obtained from these numerical simulations, a series of multi-parameter linear regression models were developed to predict the percent change in distribution factor and effective width, respectively, for girder and slab bridges with different geometrical characteristics if a refined method analysis is implemented. The regression models were limited to four parameters such that the results from regression models could be presented in table format.

The developed tables should be used as screening tools to provide guidance on the use of refined methods of analysis to improve the load ratings of bridges vulnerable to posting from previously existing load rating classifications as well as the recently introduced vehicles. Should VDOT use refined methods of analysis, there is good potential that the agency can avoid posting a substantial portion of its inventory, saving resources for more critical needs while safely keeping Virginia's bridges open for commerce and the traveling public.

17 Key Words: load rating, live load distribution factors, effective widths, refined analysis	18. Distribution Statement: No restrictions. This document is available to the public through NTIS, Springfield, VA 22161.

19. Security Classif. (of this report): Unclassified	20. Security Classif. (of this page): Unclassified	21. No. of Pages: 52	22. Price:

FINAL REPORT

PERFORMANCE CHARACTERISTICS OF IN-SERVICE BRIDGES FOR ENHANCING LOAD RATINGS: LEVERAGING REFINED ANALYSIS METHODS

Devin K. Harris, Ph.D.
Associate Professor
Department of Engineering Systems and Environment
University of Virginia

Osman Ozbulut, Ph.D.
Associate Professor
Department of Engineering Systems and Environment
University of Virginia

Abdou K. Ndong
Graduate Research Assistant
Department of Engineering Systems and Environment
University of Virginia

Muhammad Sherif
Assistant Professor
Department of Civil, Construction and Environmental Engineering
University of Alabama at Birmingham

VTRC Project Manager
Bernard L. Kassner, Ph.D., P.E., Virginia Transportation Research Council

In Cooperation with the U.S. Department of Transportation
Federal Highway Administration

Virginia Transportation Research Council
(A partnership of the Virginia Department of Transportation
and the University of Virginia since 1948)

Charlottesville, Virginia

March 2021
VTRC 21-R20

DISCLAIMER

The project that is the subject of this report was done under contract for the Virginia Department of Transportation, Virginia Transportation Research Council. The contents of this report reflect the views of the author(s), who is responsible for the facts and the accuracy of the data presented herein. The contents do not necessarily reflect the official views or policies of the Virginia Department of Transportation, the Commonwealth Transportation Board, or the Federal Highway Administration. This report does not constitute a standard, specification, or regulation. Any inclusion of manufacturer names, trade names, or trademarks is for identification purposes only and is not to be considered an endorsement.

Each contract report is peer reviewed and accepted for publication by staff of Virginia Transportation Research Council with expertise in related technical areas. Final editing and proofreading of the report are performed by the contractor.

ABSTRACT

Bridge load rating assesses the safe live load carrying capacity of an existing or newly designed structure. In addition to load rating with previously defined standard load rating vehicles, the Federal Highway Administration issued additional guidance to states related to rating requirements for all the bridges with respect to specialized hauling vehicles and emergency vehicles that must be met by the end of 2022. It is recognized that the load effects (bending moment and shear) produced by these vehicle types on certain bridge types and spans might be greater than those caused by the previous rating vehicles. Therefore, a number of bridges within VDOT's inventory may require posting when rated with these specialized vehicles.

The goal of this study was to assess the likelihood of an increase in load rating factors through refined analysis methods for the bridge classes potentially vulnerable to load ratings under consideration of the new federal regulations and when using conventional, simplified equations for load distribution factors. In particular, the study focused on the evaluation of live load distribution factors for girder bridges and effective widths for distributing live loads in slab bridges through refined analysis. Three bridge classes (simple span steel girder bridges, reinforced concrete T-beam bridges, and concrete slab bridges) were selected for this refined analysis. Girder bridges were modeled using the plate-with-an-eccentric-beam analysis approach, while plate elements were used to model slab bridges within the LARSA 4D software package. The selected modeling approaches were validated through the simulation of the bridge structures with available field-testing results from the literature. A total of 71 in-service bridges belonging to the three selected bridge classes were then modeled and analyzed to compute the load distribution factors for girder bridges or effective widths for slab bridges, and the results were compared with those obtained from the code-specified equations. Using the data obtained from these numerical simulations, a series of multi-parameter linear regression models were developed to predict the percent change in distribution factor and effective width, respectively, for girder and slab bridges with different geometrical characteristics if a refined method analysis is implemented. The regression models were limited to four parameters such that the results from regression models could be presented in table format.

The developed tables should be used as screening tools to provide guidance on the use of refined methods of analysis to improve the load ratings of bridges vulnerable to posting from previously existing load rating classifications as well as the recently introduced vehicles. Should VDOT use refined methods of analysis, there is good potential that the agency can avoid posting a substantial portion of its inventory, saving resources for more critical needs while safely keeping Virginia's bridges open for commerce and the traveling public.

FINAL REPORT

PERFORMANCE CHARACTERISTICS OF IN-SERVICE BRIDGES FOR ENHANCING LOAD RATINGS: LEVERAGING REFINED ANALYSIS METHODS

Devin K. Harris, Ph.D.
Associate Professor
Department of Engineering Systems and Environment
University of Virginia

Osman Ozbulut, Ph.D.
Associate Professor
Department of Engineering Systems and Environment
University of Virginia

Abdou K. Ndong
Graduate Research Assistant
Department of Engineering Systems and Environment
University of Virginia

Muhammad Sherif
Assistant Professor
Department of Civil, Construction and Environmental Engineering
University of Alabama at Birmingham

INTRODUCTION

According to the 2019 State of the Structures and Bridges Report by the Virginia Department of Transportation's (VDOT) Structure and Bridge Division (VDOT 2019), there are 21,173 bridges and culverts in the Commonwealth, of which, VDOT maintains 19,598. VDOT inspects more than 10,000 of these structures annually, including bridges that are less than 20 ft long and culverts that have openings that are 36 ft^2 or greater. These inspections ensure the safe and secure operation of transportation infrastructure in Virginia, as required by the National Bridge Inspection Standards (NBIS), but also provide a measure of condition state and its evolution over time. More importantly, inspection results are used as inputs to inform capacity determinations and ultimately contribute to the determination of a bridge's load rating, or safe live load carrying capacity. Thus, load ratings are critical in prioritizing maintenance operations and allocation of resources. Equally important, these ratings have a direct impact on the movement of goods and services within the Commonwealth, as postings resulting from low load ratings require vehicles exceeding these postings to find alternative paths.

In 2013, the Federal Highway Administration (FHWA) mandated state departments of transportation to rate all bridges within the state inventory for a class of vehicles called specialized hauling vehicles (SHVs) by the end of 2017 for Group 1 bridges (i.e., those bridges

whose shortest span is not greater 200 ft and load rating or rating factor is below a certain value) and by the end of 2022 for Group 2 bridges (i.e., all bridges that are not in Group 1), unless state laws preclude SHV use (FHWA 2013). In addition, the 2015 Fixing America's Surface Transportation Act (FAST Act) made certain emergency vehicles (EVs) that have considerably higher axle weight and higher gross weight than standard legal vehicles to be legal on the Interstate System and routes that are within reasonable access to the Interstate (FHWA 2016). These revisions to federal guidelines, especially pertaining to load rating of bridges for SHVs and EVs, presented a challenge that could drive some of these structures within VDOT's inventory below acceptable rating levels.

Bridge Load Rating

Based on the current evaluation methods, the operating load capacity of a given bridge is defined in terms of Rating Factors (RFs) and an equivalent tonnage for a given vehicle configuration that can traverse the bridge (AASHTO 2015). RF values at the inventory level greater than one (1.0) for the expected maximum load indicate that the structure should safely support the expected loads until the next regularly scheduled safety inspection. Otherwise, the bridge will require posting, rehabilitation, or replacement to ensure safety for the designated loading.

Equation 1 provides the general expression of the rating factor as a function of the element-level nominal capacity (R), dead load effects (D), and live load effects including dynamic amplification ($L(1+IM)$). Assuming dead loads are not subjected to major changes (e.g., overlay applications or deck rehab), variations in nominal capacity due to the existing condition state and live load effects control the corresponding rating factor. Thus, additional live load demands, as in the case of SHVs and EVs, can adversely affect the rating.

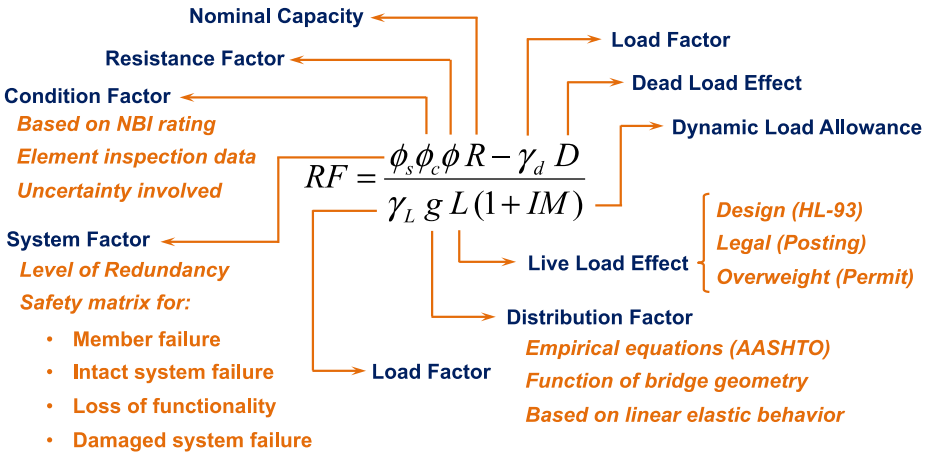

$$RF = \frac{\phi_s \phi_c \phi R - \gamma_d D}{\gamma_L g L (1 + IM)} \quad (1)$$

New Classification of Load Rating Vehicle

SHVs are defined as single unit trucks that have multiple closely-spaced axles, often with lifting or articulating intermediate axles. SHVs are primarily used in construction, waste management, bulk cargo, and commodities hauling industries. While these truck configurations

are designed to comply with the Federal Bridge Formula B, the optimization of SHVs produces heavy 4-, 5-, 6-, and 7-axle loads over a short length. As a result, SHVs can produce bending moment and shear effects on some bridge spans that are substantially larger than those from standard legal-load rating vehicles used to design and assess the bridges, such as the Type 3, 3-3, 3S2, and other state legal load configurations (Sivakumar, 2007).

Emergency vehicles also often generate load effects that are larger than those of typical legal loads and may not meet Federal Bridge Formula B. The FAST Act defined EVs as "any vehicle used under emergency conditions to transport personnel and equipment to support the suppression of fires and mitigation of other hazardous situations" (23 U.S.C. §127(r)(2)). This act amended the allowable weight limits for EVs using the Interstate System and roads "within reasonable access to the Interstate System" (FHWA, 2016). However, if states allow EVs to operate without restrictions on off-Interstate roads, then 23 CFR §650.313(c) requires that bridges along these routes must also be load rated and posted as necessary for EVs. In light of the legislation and regulation, FHWA determined that two vehicle configurations, Type EV2 and Type EV3, generally envelope the load effects of typical emergency vehicles. State departments of transportation (DOTs) can use these configurations in following the methods dictated by the AASHTO Manual for Bridge Evaluation (MBE) (2019), with the exceptions that states can assume only a single EV on a bridge at any given moment and can use a lower live load factor compared to typical rating vehicles. Furthermore, FHWA has instructed that bridges meeting certain RF conditions do not need to be rated for the new EV load types until a re-rating is warranted due to changes in conditions or other loadings. Those structures that do not meet the prescribed RF minimums should be re-rated following their next inspection, but no later than December 31, 2019.

Should a bridge have an RF value less than 1.0 upon re-rating, there are options for improving the result. In evaluating Equation 1, it is evident that opportunities for increasing a bridge's load rating can be derived from reductions in the load distribution factors (g), reductions in the dynamic load allowance (IM), and increases in the bridge capacity (R). There are opportunities for reducing the distribution factors either through refined analysis or live load testing. On the other hand, live load testing provides the only effective method for reducing dynamic load allowance (Barker, 2001; Eom and Nowak, 2001; Kim and Nowak, 1997; Yousif and Hindi, 2007). In cases where the refined analysis of the distribution factors does not sufficiently increase the RF, then load tests and perhaps additional strengthening measures may be required to mitigate weight restrictions on these bridges. Nevertheless, this project focuses on exploring potential improvements in load ratings through a reduction in live load distribution factors computed from refined methods of analysis.

Refined Methods of Analysis for Bridge Load Rating

Refined methods of analysis as described in the AASHTO LRFD Bridge Design Specifications (2017) describe a suite of methods capable of more accurately describing the behavior of a bridge system. The methods include approaches, such as classical plate analysis, finite strip method, and finite element analysis, where these methods account for the complex interactions within a structural system that are often simplified in the design process. In recent years, the finite element method and the three-dimensional stiffness method have become the

most applicable forms of refined methods of analysis. With advances in computational power, these approaches have allowed for bridges to be represented in their three-dimensional configuration, subjected to variable loading scenarios, and analyzed efficiently, allowing these approaches to become more commonplace in the bridge community. An extensive body of literature on these refined methods of analysis already exists, and therefore will only be referenced briefly throughout this report.

PURPOSE AND SCOPE

The primary purpose of this study is to evaluate the potential for reducing the number of bridges within VDOT's inventory that will require posting by leveraging the general form of the AASHTO load rating factor equation through refined analysis methods.

The scope of this investigation includes an evaluation of the bridge populations potentially vulnerable to load ratings under consideration of the new federal guidance and an assessment of the potential improvement in RFs that could be achieved through refined analyses. Within this scope, the bridge types evaluated were based on the VDOT inventory of bridge structures that have an RF less than 1.0. The research scope does not aim to increase the rating factor for any given bridge, but instead define the characteristics of structural systems that have the best potential for achieving an RF value greater than or equal to 1.0 should a refined analysis be conducted.

METHODS

Overview

This research project consists of four tasks to achieve the main research objective:

1. Detailed literature review and current state of practice
2. Selection of the bridge classes and population to be evaluated
3. Selection of the refined analysis methods
4. Refined analysis of bridge classes and evaluation of load distribution behavior

Literature Review

The research team compiled a literature review to document the relevant information related to the assessment of load distribution behavior of bridges using refined analysis and the effects of SHVs and EVs on bridge load ratings. The literature search included not only published articles in academic journals and proceedings, but also research reports developed by other state departments of transportation (DOTs).

Selection of the Bridge Classes and Population to Be Evaluated

To select the bridge classes to be evaluated in this study, bridges within the VDOT inventory having an RF below 1.0 for all AASHTO SHVs (SU4, SU5, SU6 and SU7) were first identified. The bridge ratings were provided to the research team in two different databases; the state database and the district-level database. The state database ratings were updated with the districts' ratings. Railroad bridges, pedestrian bridges, and culverts were excluded from the database because the focus of this investigation was highway bridges. The database had the ratings for single, semi, SU4, SU5, SU6, and SU7 trucks for each bridge. The tonnage ratings for SUs were normalized for the weight of SU4, SU5, SU6, and SU7 trucks, respectively.

The minimum RF based on the SU truck ratings of each bridge was used to categorize the bridges. Bridges with an RF < 1.0 were classified based on their structural type and construction material. These bridges were also grouped into three categories based on route type: interstate, primary, and secondary. Within the databases provided, 19% of the bridges had not been rated for SHVs at the time of this analysis. These bridges without a rating factor for SU trucks were also categorized based on their structural type and construction material, with the goal of understanding their primary make-up relative to all bridges with RF < 1.0.

Considering the population of bridges affected by the SHV ratings and route importance, as well as the distribution of bridges without SHV ratings, three bridge classes were selected for the evaluation using refined methods of analysis. The structural characteristics of each bridge, such as span lengths, number of lanes, and skew for the selected three bridge classes, were analyzed to obtain representative examples to be modeled and analyzed using selected refined analysis methods.

Selection of Refined Analysis Method

In this investigation, a key component in the analysis was the selection and deployment of an appropriate refined method of analysis. These methods of analysis ultimately determine accuracy of the loading and load sharing behavior of the structural system. Depending on the level of refinement, a structural analysis can be described as one-dimensional (1D), two-dimensional (2D) or three-dimensional (3D). The classification of the analysis is not necessarily correlated with the type of elements or geometry considered in the analysis. Following the definitions provided in Adams et al. (2009), an analysis can be described as 1D when the resultant quantities, such as moments, shears, and deflections, are a function of only one spatial dimension. When two or three spatial coordinates are used to describe the results, then the analysis can be described as 2D or 3D analysis, respectively.

A 1D analysis assumes the structure can be modeled using a single series of line elements and with the resultants distributed transversely through empirical equations. This type of analysis cannot explicitly account for geometry and element stiffnesses in the evaluation of load sharing behavior. This 1D analysis approach is the basis of the load sharing behavior (load distribution factors) used for design with the beam line approach within the AASHTO LRFD Bridge Design Specifications (2017). 2D methods of analysis methods are the most commonly used approaches to model slab and slab-on-girder bridges when 1D analysis is not appropriate. For 2D methods,

the plane of the deck surface is typically the geometric reference for the analysis with the planar or line element used to describe the behavior of the bridge system. Using this same approach, a 3D model can effectively be reduced to a 2D analysis (grillage or eccentric beam) while still including the effects of girder eccentricity or transverse components such as cross-frames. 3D methods of analysis require the critical member of the model to be explicitly created, positioned, and connected. For example, in a 3D analysis of a beam-girder bridge, the girder flanges and webs, cross-frames and diaphragms, and bridge deck would be modeled using separate elements.

Considering the computational effort needed to extract the desired response quantities and the complexities in its implementation, a 3D analysis was not explored in this study. Instead, the study focused on the use of 2D methods of analysis that could be efficiently implemented in LARSA 4D, VDOT's preferred finite element analysis platform. For the refined analyses of slab-on-girder bridges, two modeling approaches were evaluated: 1) basic grid analysis, and 2) plate with eccentric beam (PEB) analysis. For the refined analyses of slab bridges, two modeling approaches were evaluated: 1) basic grid analysis, and 2) 2D plate analysis methods.

Basic Grid (Grillage) Analysis

The basic grid analysis method, which is often also called grillage analysis, involves the modeling of the bridge as a skeletal structure made up of mesh of beams in a single plane. Beam elements are used to model the behavior of the girders in the longitudinal and transverse directions. Properties of the longitudinal grid lines are determined from section properties of the girders and the portion of the slab above them calculated about the centroid of the composite transformed section. Transverse grid lines are added at cross-frame locations and other additional locations with the longitudinal grid to form an idealized mesh. Additional grid patterns can be integrated to allow for refinement of load placement and inclusion of secondary members such as parapets. The basic grid analysis method is simple and easy to implement, but has some limitations. This method cannot model physical phenomena such as the shear transfer between girders and deck slab, and warping torsion. These limitations come from the fact that, in grillage analysis, structural members lie in one plane only.

Plate with Eccentric Beam Analysis

The plate with eccentric beam analysis method is an extension of basic grid analysis, where the girders and deck slab are modeled separately. This model is capable of including physical behavior, such as composite action and the eccentricity effect between the slab deck and the girder. Using this modeling approach, it is also possible to capture shear lag effect, which refers to the influence of in-plane shear stiffness on normal stress distribution due to bending. The analysis method utilizes the non-composite section properties of two elements to model the degree of composite action by applying the rigid links between the centroid of the girder and the mid-surface of the slab. The girders are modeled using beam elements and the concrete slab deck is modeled as a set of shell elements. By considering at least two shell elements between each line of girders, shear lag effects can be accounted for. Cross-frames or bracing can be modeled using beam elements that represent the entire cross-frame section.

2D Plate Analysis

The 2D plate analysis method uses a 2D finite element method with plate elements to represent the bridge slab. Plate elements are developed assuming that the thickness of the plate component is small relative to the other two dimensions. The plate is modeled by its middle surface. Each element typically has four corners or nodes. Following general plate theory, plate elements are assumed to have three degrees of freedom at each node; translation perpendicular to the plate and rotations about two perpendicular axes in the plane of the plate. The typical output includes the moments (usually given as moment per unit width of the face of the elements) and the shear in the plate. This form of output is convenient because the moments may be directly used to analyze load sharing behavior within the deck. The main disadvantage of plate elements is that they do not account for the forces in the plane of the plate, resulting in the in-plane stiffness being ignored in the analysis.

Modeling Validation

The performance of these methods was evaluated by considering important aspects such as the efficiency of model development, accuracy of the results, detail required, and computational effort needed. While computational models are gaining traction as a common tool in structural analysis, validation of modeling approach is still necessary to create confidence in the derived results. To achieve this confidence, the three refined analysis approaches used in this study were validated using the experimental results provided in the literature from the field testing of in-service bridge structures (Harris, 2010; Harris et al, 2020; Eom and Nowak, 2001).

The structures analyzed included one steel girder bridge, one reinforced concrete T-beam bridge, and one reinforced concrete slab bridge. All models developed in the validation were created using LARSA 4D, based on the geometric details and loading patterns prescribed in the literature. A comprehensive description of the model development is not presented in this report, but details of the bridge geometries and loading patterns can be found in the original references (Harris et al, 2020, Eom and Nowak, 2001). For the model validation study, the primary objective was to reasonably represent the behavior described in the experiments with the models developed in this study without model tuning or calibration for uncertainties surrounding boundary condition, constitutive properties, or condition state. Therefore, the models were expected to follow behavior characteristics, but were not expected to match results exactly.

Steel Girder Bridge

The steel girder bridge selected for validation was located on Stanley Road over I-75 (S11-25032) in Flint, Michigan. The structure consisted of a three-span structure with simple supports and a total length of 285 ft. An 8-in reinforced concrete deck was supported by seven steel plate girders with a transverse spacing of 7.25 ft. The bridge was part of a comprehensive load testing program conducted by Nowak and Eom (2001) in collaboration with the Michigan DOT. Only the second span of the structure was chosen for validation in this study. This span was 135 ft long with a clear span of 126 ft between pin and hanger connections. The loads applied to the model came from the Nowak and Eom study and were representative of the 11-axle design trucks common to the state of Michigan. For simplicity, only the scenarios of pin–roller and pin–pin were analyzed, with no attempt to calibrate the rotational restraint of the

supports, a procedure that was employed by Eom and Nowak (2001). This approach was adopted since the intent of the investigation was to evaluate performance of different methods for determining lateral load distribution rather than an exercise in model calibration. Deflection results from this study and a validation study by Harris (2010) were used for model validation.

Reinforced Concrete T-beam Bridge

The Flat Creek Bridge carried Route 632 over Flat Creek located in Amelia County, VA. There were five simple spans, each 42.5 ft long, for a total length of 212 ft with no skew. Each span was 24 ft wide and consisted of four longitudinal T-beams. Each exterior T-beam had a vertical stem with a width of 14 in and a depth of 32 in. Each interior T-beam had a vertical rectangular stem with a width of 16 in and a depth of 32 in, and a wide top flange of 7.5 in thick. The wide top flange was the transversely reinforced deck slab (Harris et al., 2020). The strain results of the field load tests were used to verify the refined analysis models.

Reinforced Concrete Slab Bridge

The Smacks Creek Bridge carried Route 628 over Smacks Creek in Amelia County, VA. The superstructure comprised of two 32-ft long, 21-in thick, simply-supported reinforced concrete slabs that had a 15° skew. The deck had 12-in diameter voids oriented in the direction of traffic, spaced 18 inches apart (Harris et al., 2020). The strain results of the field load tests were used to verify the finite element models, which used equivalent cross-sections for the voids.

Refined Analysis of Bridge Classes and Evaluation of Load Distribution Behavior

In this task, refined methods of analysis were used on a population of bridges within VDOT's inventory to evaluate changes in measured response as compared to the design assumption behaviors. More specifically, these results from the analysis explored the impact of these refined methods of analysis on describing the load sharing behavior as compared to the AASHTO LRFD simplified equations for live load distribution factors and effective widths. After the performance of the two modeling approaches described earlier was assessed for girder and slab bridges, the plate with eccentric beam modeling approach was used to determine load distribution factors for the girder bridges and a 2D linear elastic plate analysis was employed for the refined analysis of slab bridges. A total of 21 steel girder bridges, 25 T-beam bridges, and 25 slab bridges were selected for evaluation using the refined method of analysis. These bridges were selected from the VDOT inventory within these three classes of structures and were considered representative of the geometric characteristics of bridges vulnerable to the low load ratings due to the federal mandates. For each of the modeling approaches, a general overview of the model development, load application, results extraction, and baseline comparison approach are described in the following subsections. Additionally, the process automation for the model development and result extraction is briefly discussed.

Plate With Eccentric Beam Modeling

Model Development

The first step of a refined analysis using the plate with eccentric beam approach involved creating a two-dimensional finite element model, which was then used to compute a more accurate live load distribution factor. The depth of the structure was accounted for by locating the deck slab and longitudinal beams at their respective centroids, such that girders were eccentric to the deck plate. The PEB model located beam elements along the centroids of longitudinal girder lines. Beam elements were also used to connect the longitudinal elements transversely at cross frame/diaphragm locations when applicable. Plate elements were used to model the concrete deck over the entire length. The number of elements used to model the girders and the deck were interrelated, as the two were connected at nodal locations. A typical model for a steel girder bridge is shown in Figure 1. All the bridges were simply supported and their boundary conditions were modeled using pin-roller supports.

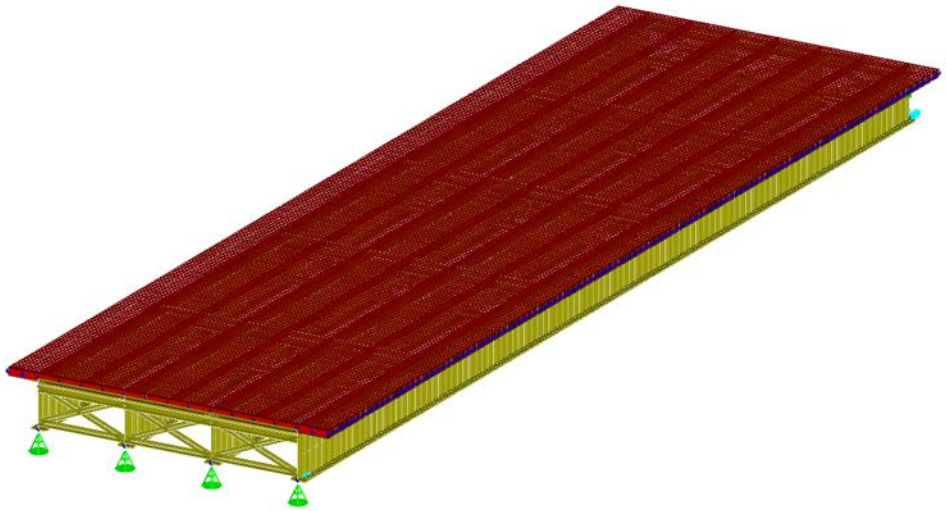

Figure 1. Finite Element Model of a Typical Steel Girder Bridge

Application of Loads

The developed models were subjected to live loads representing the AASHTO vehicles of interest to this study. For the analyses, only static loadings were considered, as these are primary drivers in the load sharing behavior of a bridge. For each vehicle represented in the analysis, wheel loads were modeled as concentrated loads and applied to the corresponding nodal coordinate on the model. In the case that a wheel load did not match a model node, the load was assigned to the nearest model node. The loadings were positioned longitudinally on the bridge using an influence line approach to generate the maximum longitudinal response, but the transverse position(s) of the load was determined through an iterative solution by systematically moving the loading every two feet in the transverse direction of the bridge.

Extraction of Load Distribution Factors

The loads effects, namely shear and moments, were obtained from refined analysis and used for the computation of live load distribution factor, *g*. In particular, load fraction analysis approach was employed to compute the distribution factors for both moment and shear of each girder of the composite sections (Harris, 2010). This technique is based on Equation (2), where $R_{max,j}$ represents the maximum moment or shear of the j^{th} girder and N_{trucks} is the number of trucks. Alternative forms of the live load distribution factor equation are presented as *mg*, where *m* is the multiple presence factors which is taken as 1.2, 1.00, 0.85, and 0.65, respectively, for one, two, three, and four or more lanes loaded, as defined in the AASHTO LRFD Specification (2017).

$$g = \frac{R_{max,j}}{\sum_{j=1}^{\#girders} R_{max,j}} \cdot N_{trucks} \tag{2}$$

2D Plate Analysis

Model Development

The first step of the refined analysis using 2D plates involved creating a two-dimensional finite element model, which was then used to compute the portion of the slab's effective width in resisting the applied load. Without beam elements, plate elements made developing the model geometry that represented a slab bridge relatively simple. The concrete slab was modeled using plate elements with four nodes. The mesh size in each bridge model was set to be equal to the half of the slab thickness or less. Pin and roller supports were set as boundary conditions for the developed models.

Application of Loads

The live load application approaches used in the slab-on-girder bridges were also used in refined analysis of slab bridges. To simplify live load application to the deck in the model, the size of the elements was selected to eliminate the partial loading of some finite elements, i.e. the tire contact area preferably matched the area of one or a group of elements.

Extraction of Effective Width

The stress results obtained from the 2D plate model was used to create a plot of the longitudinal stress versus transverse location, from which the effective slab width was determined. These plots were created using both a single truck and two trucks side-by-side located at different transverse locations. The absolute maximum stress due to the maximum bending moment at any given time was used as the reference for determining the critical effective width. The stress values across the transverse direction of the deck were then extracted and organized into a distribution plot. A typical stress distribution plot is shown in Figure 2.

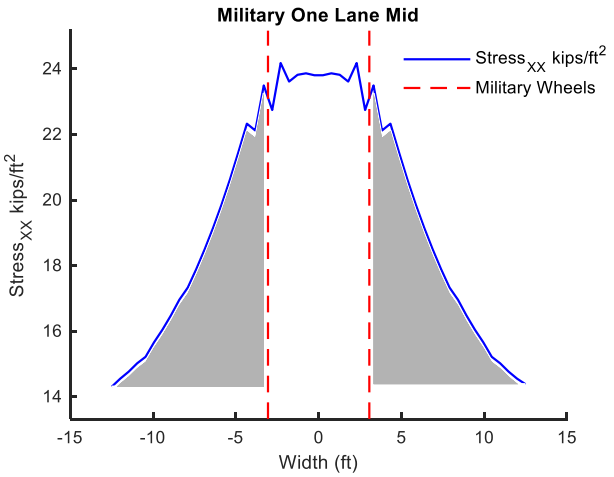

Figure 2. Typical Transverse Stress Distribution Plot

An idealized stress (or strain) distribution would have a relatively constant peak value between the truck wheels, and would decrease to zero further away from the wheels as shown in Figure 3. This non-uniform stress is a result of shear-lag and the concept of effective width was developed to simplify the evaluation of slabs that exhibit shear lag. The effective width section has a constant stress across its width and creates the same total effect as that caused by the actual stress distribution (Chiewanichakorn et al., 2004). Figure 3 conceptually illustrates how the transformed areas are determined for a wheel pair by maintaining a constant peak and determining the width that has the same area under the curve.

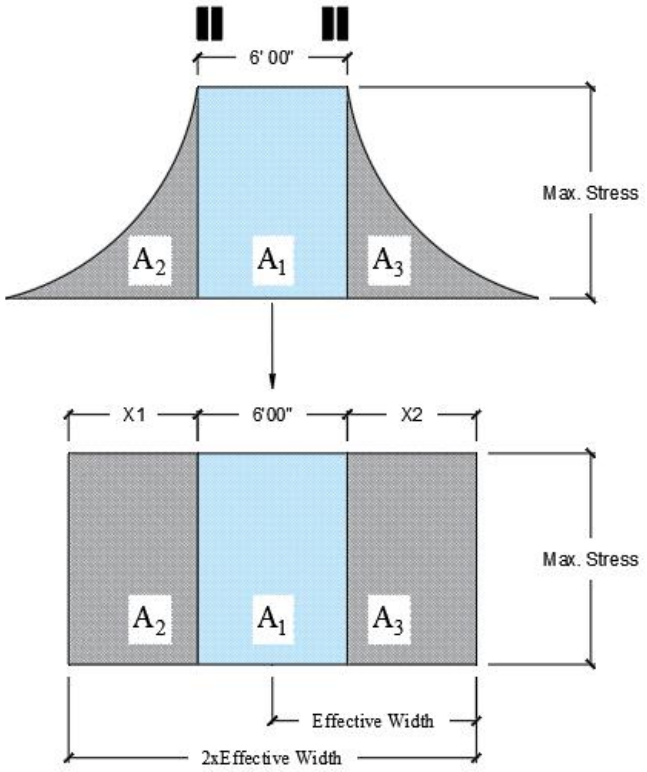

Figure 3. Idealized Stress Distribution and Effective Width Representation

Process Automation

Initially, the bridge geometry including section properties were specified in LARSA 4D (LARSA, Inc.). A mesh was generated based on the dimensions of the bridge as well as taking into consideration the computational time and the application of load. To apply the truck loads and minimize the amount of finite element data required, a MATLAB (Mathworks, Inc.) script was developed. A database with the axle loads of common trucks was identified and generated in MATLAB. The MATLAB script had two main tasks: (1) read and identify the nodes associated with the truck loading for each truck and (2) write a modified LARSA 4D file with the applied loads for each scenario. Finally, the analysis was conducted using the modified LARSA 4D file, and the results were extracted for each case. For the girder and slab bridges, a flowchart of the procedure for determining the load distribution factor and effective width is shown in Figures 4 and 5, respectively.

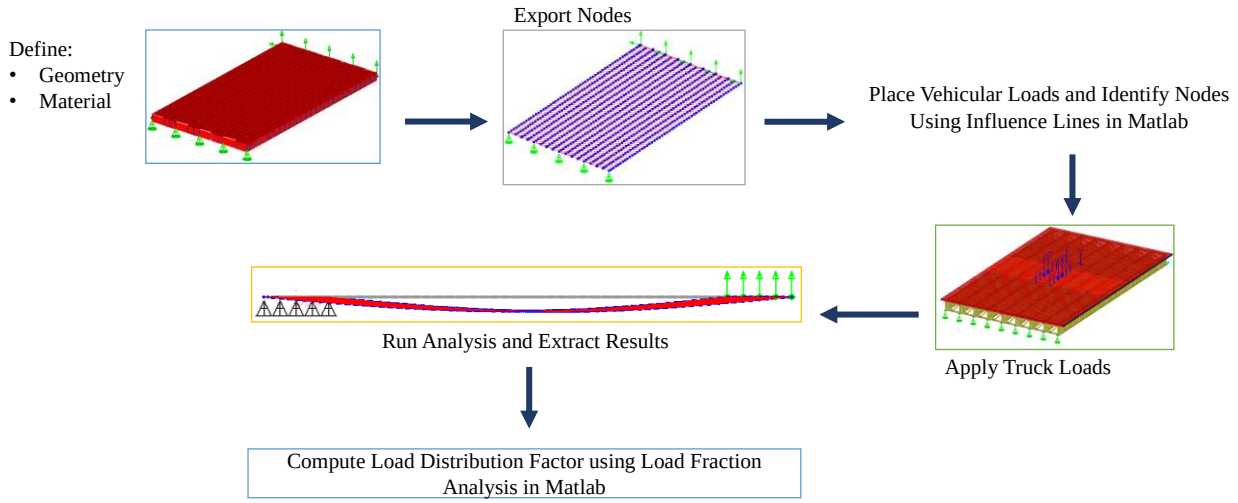

Figure 4. Flowchart of the Procedure Used for the Determination of the Live Load Distribution Factor

The AASHTO trucks considered in the analyses were the HL93-Design Tandem, the HL-93/HS20-44 Design Truck, and the SU7 Legal Truck. A number of load cases needed to be tested in the longitudinal and transverse positions to determine the maximum effect generated at a specific location using the selected trucks. The truck positions that produced the maximum moment and shear in the longitudinal direction were first determined. Then, three transverse positions were considered for both moment and shear effects: (1) a truck placed 2 ft from the curb of the parapets; (2) a truck placed at the quarter length of the clear road width; and (3) a truck placed in the mid-transverse position of the bridge. The same was repeated for two trucks. Therefore, a total of 36 load cases were considered for each bridge.

Prediction Models

Results derived from the refined methods of analysis provided the foundation describing the characteristics that influenced the load sharing behavior within the selected bridge categories. With a goal of understanding where potential improvements in rating factor could be achieved, an understanding of the bridge parameters driving this load sharing behavior was necessary. However, the pool of bridges was limited to around 20 to 25 bridges per category, which would

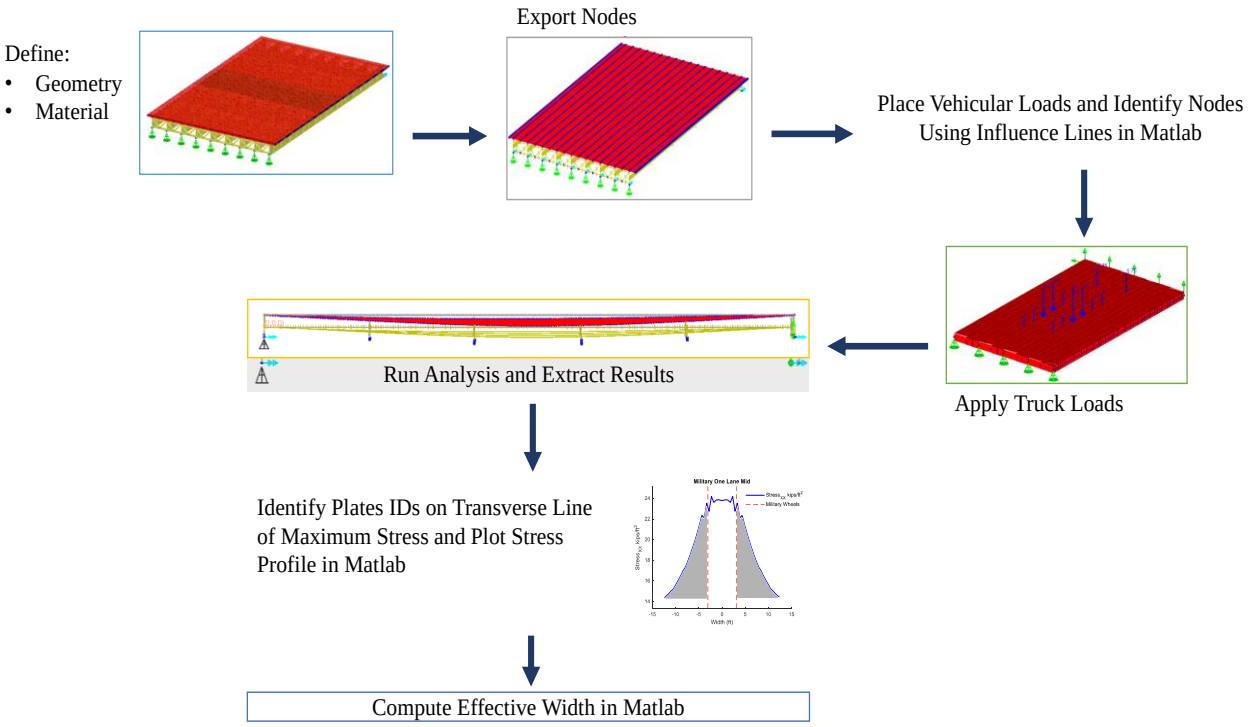

Figure 5. Flowchart of the Procedure Used for the Determination of Effective Width

not be expected to elucidate any trends. As such, the percent changes in distribution factors and effective width, of these bridges derived from the refined analyses provided the basis to evaluate the geometric parameters driving the structural response and develop linear regression models based on these parameters.

The developed models utilized a best subset regression approach, which is a method that regresses multiple variables while simultaneously eliminating those that are not relevant. Best subset regression is also known as "all possible regressions" and "all possible models". This regression approach tested all possible combinations of the independent variables that were specified. After fitting all of the models using R (R Core Team, 2013), a commercial statistical analysis software package, the best models were selected using the R-squared as the statistical criteria (Hawkins and Galpin, 1986). The outcome was a presentation of the best-fit models with increasing number of independent variables up to the full model size that considers all the variables. In this study, to improve the accuracy of the prediction models, the regression equations were established considering the interaction among the selected parameters. While multi-parameter regression has the capability to extract models that best fit the dataset, the models developed in this study were limited to four parameters and their associated interactions. The choice of having four parameters in the regression models was a practical decision informed by the goal of developing look-up tables that could be easily referenced. The use of more than four parameters resulted in improved predictions, but at the expense of requiring complex visualizations. In addition, eighty percent of the observations were used as a training set, while the remaining twenty percent were used to test the models.

Comparison with AASHTO LRFD Bridge Design Specifications

For all analyses, comparisons of performances are described relative to the design reference of the AASHTO LRFD Bridge Design Specifications. More specifically, for girder bridges, AASHTO LRFD lateral load distribution factors for moment and shear served as the references for comparison, while the effective width defined in the AASHTO LRFD specifications served as the reference for slab bridges. The distribution factors for moment and shear for the exterior and interior girders and the effective width for slab bridges were computed from the refined analyses and compared with those computed using the AASHTO LRFD equations. For girder bridges, based on the results of the analysis for each bridge within the evaluation population, the cumulative worst case (i.e. largest distribution factor) were compared with the AASHTO LRFD design reference as a percent change using Equation 3,

$$\Delta DF\,(\%) = \frac{DF_{model} - DF_{AASHTO}}{DF_{AASHTO}} \cdot 100 \tag{3}$$

where:

DF_{model} = the load distribution factor (DF) computed using refined analysis
DF_{AASHTO} = the DF computed from the AASHTO LRFD Specifications
ΔDF = the percent change in the DF when computed using refined analysis versus the AASHTO LRFD specifications.

Note that a negative change indicates that the refined analysis method showed a bridge with the given parameters was more effective in distributing the load than originally predicted and thus yielded an improvement in the load rating relative to the AASHTO LRFD design basis.

For slab bridges, the smallest effective width obtained for either single lane loading or multi-lane loading cases was compared with the effective width computed using the corresponding AASHTO LRFD equation as a percentage change using Equation 4,

$$\Delta EW\,(\%) = \frac{EW_{model} - EW_{AASHTO}}{EW_{AASHTO}} \cdot 100 \tag{4}$$

where:

EW_{model} = the effective width (EW) computed using refined analysis
EW_{AASHTO} = EW computed using AASHTO LRFD Specifications
ΔEW = the percent change in the DF when computed using refined analysis versus the AASHTO LRFD specifications.

Note that a positive change in effective width indicates an improvement in the rating factor for slab bridges. The results of changes in effective width are presented for single and multi-lane loading cases separately for slab bridges analyzed through refined analysis methods. However, the results from the worst loading case, i.e. smallest effective width computed for single and multi-lane loading cases, were considered in the development of prediction models.

As can be seen from the load rating equation provided in Equation 1, the rating factor is inversely proportional to the distribution factor. Therefore, taking all the variables except the distribution factor in the load rating equation as the same, the percent change in the rating factor (ΔRF) computed from refined analysis versus that from the AASHTO LRFD Specifications can be obtained as:

$$\Delta RF\,(\%) = \frac{RF_{model} - RF_{AASHTO}}{RF_{AASHTO}} \cdot 100 = \left(\frac{RF_{model}}{RF_{AASHTO}} - 1\right) \cdot 100 \tag{5}$$

or

$$\Delta RF\,(\%) = \left(\frac{DF_{AASHTO}}{DF_{model}} - 1\right) \cdot 100 \tag{6}$$

where, RF_{model} and RF_{AASHTO} denote the rating factor computed using refined analysis and AASHTO LRFD Specifications, respectively.

RESULTS AND DISCUSSION

Literature Review

This literature review is organized into two main sections. First, the review of the literature on the use of refined analysis methods in evaluation of load distribution factors and bridge load rating is provided. Then, the impacts of the SHVs and EVs on the load rating process are reviewed.

Refined Analysis for Load Distribution and Load Rating

The analytical expressions to determine the load distribution factors in the AASHTO LRFD Specification were developed as a result of NCHRP 12-26 project (Zokaei, 1991), where extensive parametric studies on straight, single-span bridges were conducted using finite element analysis. The results from the study were considered as a better representation of load distribution in bridge structures compared to "S-over" equations in the AASHTO Standard Specification. However, AASHTO LRFD formulas were developed by making a set of assumptions and therefore have some limitations. For instance, the girder spacing was assumed to be uniformly distributed and all girder characteristics were taken to be the same. It was also assumed that the HS-20 design vehicle governed the distribution behavior. In addition, the effects of some important parameters such as cross-frames, diaphragms, and deck cracking in load distribution were not considered in the development of these expressions.

Since the development of AASHTO LRFD load distribution expressions, a number of studies have been conducted to investigate load distribution behavior of girder bridges and slab bridges through refined analysis. These studies evaluated the effects of various parameters on the load distribution factors and compared their findings with the AASHTO Standard and LRFD approaches. These studies highlight the current state of practice regarding the application of

refined methods of analysis to better describe load sharing behavior, but also emphasize the variability of impact of bridge parameters on these same behaviors.

Girder Bridges

Chung et al. (2006) investigated the influence of cross bracings, parapets, and deck cracking on load distribution factors of steel girder bridges. They developed 3D finite element models of 9 in-service bridges in Indiana using ABAQUS. Shell elements were used to model the concrete deck, while the steel girders and bracing elements were modeled using beam elements. The composite action between the girder and deck was modeled by rigid links. The models were loaded with the AASHTO HS20 design truck to obtain the live load distributions. The study found that when the load distribution factors were calculated using finite element models that consider lateral bracings, the factors decreased by up to 11% compared to those computed using finite element models that included only primary members. A decrease up to 25% was observed when only parapets were considered in the models. When both lateral bracing and parapets were added to the models, the load distribution factors were 17-38% less than those obtained using the models with only primary members. On the other hand, considering longitudinal cracks on the concrete deck increased the load distribution factors by 17% while the transverse cracks had a negligible effect on the load distribution behavior.

Harris (2010) comparatively evaluated a number of methods used by researchers to determine load distribution factors for girder bridges. The load distribution factors were computed using an approach based on either the load fraction method or the beam-line method. The finite element model of a bridge validated through the field-testing results was used to determine member response including strains, deflections, and moments, which were then used to determine load distribution factors using variations of the load fraction and beam-line methods. The results demonstrated that both of these methods were effective for determining load distribution factors, but proper selection and use of appropriate member response variables was critical.

Catbas et al. (2012) developed 3D finite element models of 40 reinforced concrete (RC) T-beam bridges and evaluated the load distribution factor by analyzing the moment values under HL-93 design truck loads. The models included 3D solid elements for concrete and frame elements for reinforcing bars. The effects of secondary elements such as diaphragms, parapets, and sidewalks were not considered. The study found interior girder moment demands decreased at least 30% when they were computed through finite element analysis rather than AASHTO LRFD equations. The authors proposed a method to compute the load distribution factors using parameters obtained from a simple dynamic test and measured skew angle. Field testing on four in-service T-beam bridges was conducted to evaluate the load distribution factors through both the proposed approach and the detailed field-calibrated finite element models. The rating factors for these bridges were also computed using the AASHTO LRFD approach. The average ratio of the load ratings computed by fully calibrated models to AASHTO load ratings was 3.32, while the average ratio of the load rating estimated by the proposed approach to AASHTO load ratings was 1.40. These outcomes demonstrated the potential benefits derived from the proposed approach, which still resulted in improved rating factors compared to AASHTO approach while remaining conservative compared to the fully calibrated finite element modeling approach.

Nouri and Ahmedi (2012) assessed the effect of skew angle on the load distribution behavior of continuous two-span steel girder bridges. They performed finite element analysis of 72 bridges with varying parameters under AASHTO HS-20 loading in SAP 2000. The models employed shell elements for concrete deck, beam elements for girders, and rigid link elements to connect shell and beam elements for representing the composite action between the deck and girders. The results showed that the moment demands for interior and exterior girders decreased up to 33% when the skew angle varied from 0° to 45°. The shear forces at the pier support decreased for interior girders, but increased for exterior girders with increasing skew angle. The study also concluded that the AASHTO LRFD approach overestimated the moment and shear distribution factors up to 45% when the skew angle was over 20°.

Snyder and Beisswenger (2017) studied shear rating factors for prestressed concrete beams using refined analysis in a project funded by Minnesota DOT. They analyzed 50 prestressed concrete bridges through 2D grillage models and computed the live load distribution factors considering the location-based load distribution of each axle along the span. They found an average of 7% decrease in live load distribution factors. This refined analysis increased load ratings for all of the analyzed bridges by an average of 16%.

Dymond et al. (2019) conducted a parametric study to evaluate the shear distribution factors for prestressed concrete girder bridges without any skew. They found that the ratio of longitudinal stiffness (composite girder longitudinal moment of inertia divided by cube of span length) to transverse stiffness (transverse deck strip moment of inertia divided by cube of beam spacing) plays an important role in shear distributions. They reported that when the stiffness ratio was less than 1.5, the live load shear demands calculated by refined analysis were lower than those computed by the AASHTO LRFD approach, while the refined analysis and AASHTO approximation lead to similar results if the stiffness ratio was between 1.5 and 5.0. However, the refined analysis produced higher shear demands for bridges with a stiffness ratio greater than 5.0.

Slab Bridges

Amer et al. (1999) conducted a parametric study to assess the influence of span length, bridge width, slab thickness, and edge beams on the effective width of solid slab bridges. A basic grid analysis approach was used to model 27 slab bridges with varying parameters. The models were loaded with the AASHTO HS20 design truck. They concluded that the span length and edge beams were the main parameters that influenced the effective width. The effective widths computed by grillage analysis were always higher than those computed with the AASHTO LRFD approach. Three bridges were experimentally tested and the effective width for each bridge was computed based on measured strains. Results indicated that the effective width of these bridges computed by grillage analysis was 14% higher on average than those computed by AASHTO equations, while the effective widths based on field tests were 40% higher on average than AASHTO effective width calculations. Therefore, while the AASHTO calculations were the most conservative, the proposed methods were about 25% more conservative than what has been observed in actual load tests.

Mabsout et al. (2004) studied the load distribution behavior of single span, simply-supported reinforced concrete slab bridges through parametric analysis. Finite element analyses of 112 bridges with varying span lengths, number of lanes, slab thickness, and edge condition

were performed using SAP 2000. The models used shell elements to represent the concrete slab. Various loading conditions were considered using the AASHTO design truck. The maximum longitudinal moments obtained from the models were compared with those computed through AASHTO Standard and LRFD Specifications. They concluded that the AASHTO LRFD Specification overestimated the bending moments for slab bridges.

Jauregui et al. (2007) investigated the load distribution behavior of an in-service RC continuous slab bridge in a project funded by the New Mexico DOT. A finite element model of the bridge was developed in SAP 2000 using shell elements to model the slab. The model was validated using strain measurements obtained from a diagnostic load test. They found that the effective width increased by 26% and 22% for positive moment and 13% and 11% for negative moment for the exterior and interior spans, respectively, compared to the AASHTO LRFD approach.

Davids et al. (2013) conducted refined analysis of 14 in-service slab bridges maintained by the Maine DOT. The analyses were performed using a finite element analysis software, SlabRate, developed and validated by the researchers. The software employed quadratic plate elements to model the slab. The finite element analyses resulted in an average of 25.5%, 25.7%, and 26.3% increase in rating factors for the HL-93 truck, HL-93 tandem, and AASHTO notional load, respectively, compared to the AASHTO LRFD approach.

Impacts of SHVs and EVs on Bridge Load Rating

There have been only a few published studies related to the effects of SHVs and/or EVs on bridge load ratings. Islam (2018) discussed a study where 187 in-service bridges owned by Ohio DOT were load rated by either load factor rating or load and resistance factor rating for both Ohio legal trucks and SHVs. The bridges selected for the study included concrete slab bridges, prestressed concrete I-girder and box-girder bridges, and steel girder bridges. The results showed that almost all of the evaluated bridges that had an RF greater than 1.35 for Ohio legal loads also had an RF greater than 1.00 for SHV loads.

Selection of the Population of Structures to Be Evaluated

After applying filters to focus on only highway bridges, there were a total of 11,440 bridges in the database obtained from VDOT. Figure 6 (a) shows the distribution of bridges with an RF < 1.0 for either inventory rating or when they are rated with SU trucks, for each of three route types. The RF values are grouped into four ranges: (i) < 0.3, (ii) 0.3 – 0.5, (iii) 0.5 – 0.7, and (iv) 0.7 – 1.0. 81% of the bridges with a RF < 1.0 are located along secondary routes. For those secondary route bridges, 49% of bridges had an RF below 0.7. 89% of primary route bridges and all interstate bridges with an RF < 1.0 had an RF over 0.7. Figure 6 (b) shows the distribution of all bridges with an RF < 1.0 based on structural type. It can be seen that most of the bridges were categorized as girder bridges (74%) and slab bridges (22%).

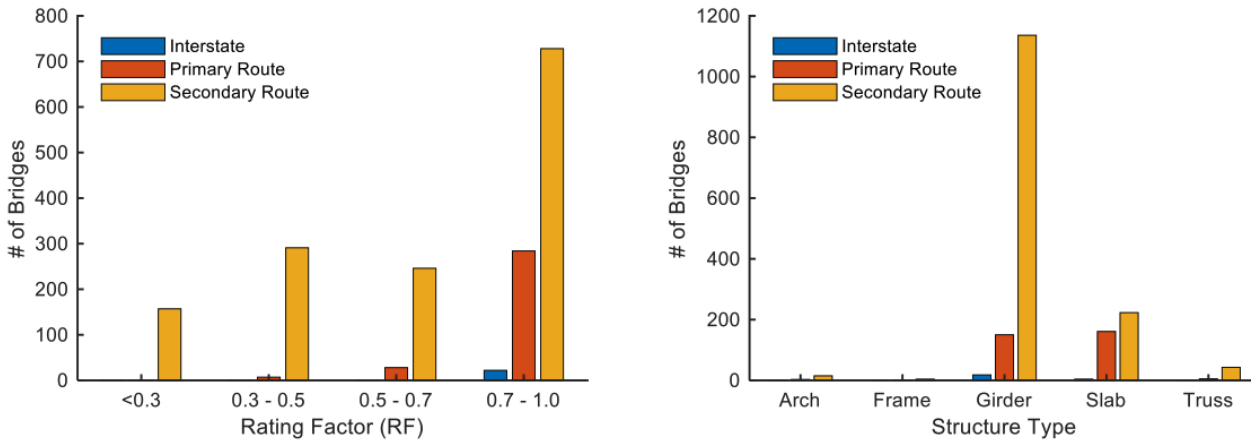

(a) **(b)**

Figure 6. Bridges with RF < 1.0 Categorized Based on: (a) rating factor; (b) structure type

Figure 7 (a) shows the distribution of slab bridges with an RF < 1.0 for either inventory rating or when they are rated with SU trucks, organized by construction materials and route type. Almost all of these bridges are concrete slab bridges. There are 4, 161, and 221 concrete bridges with an RF < 1.0 on interstate, primary, and secondary routes, respectively. Figure 7 (b) shows the distribution of girder bridges with an RF < 1.0 distinguished by construction material and route type. Although a large number of these bridges are steel girder bridges with timber (wood) deck, almost all of these bridges are located on secondary routes and were not prioritized for this study. An enlarged view of just the concrete and steel girder bridges with concrete decks distinguished by route type is shown in the inner plot of Figure 7 (b). For concrete girder bridges, 50% of the bridges are located on either primary routes or interstates. Similarly, 48% of steel girder-concrete deck bridges are located on either primary routes or interstates.

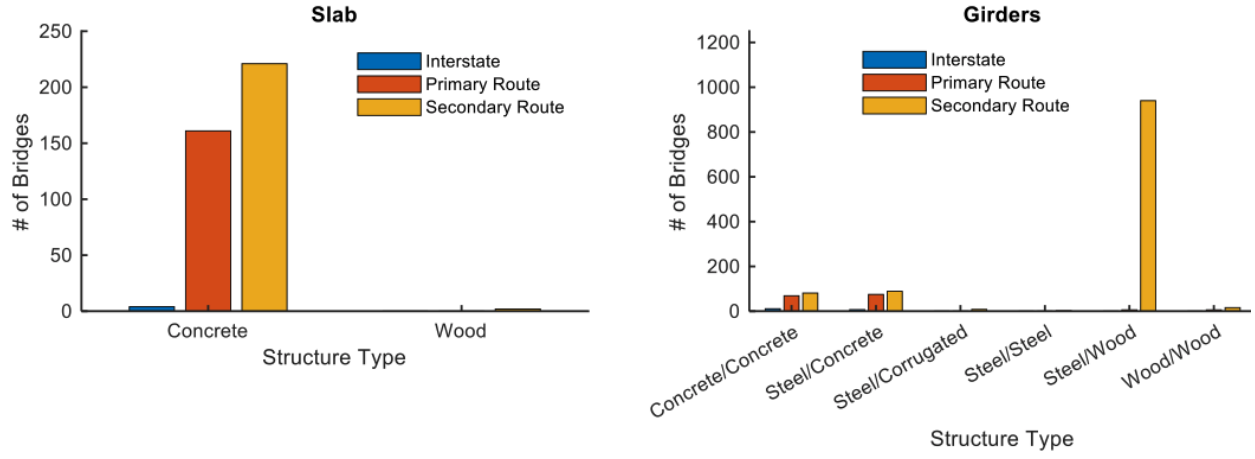

(a) **(b)**

Figure 7. Bridges with RF < 1.0 Categorized According to Construction Material: (a) slab bridges; (b) girder bridges

Figure 8 (a) and (b) show the distribution of concrete and steel girder bridges, respectively, with an RF < 1.0, for various superstructure and route types. For the concrete girder

bridges, 68% of the bridges are reinforced concrete T-beam bridges. 53% of these T-beam bridges are located on primary routes, while 45% are on the secondary routes. For steel girder bridges, 69% are simple span girder bridges. About 3% of these simple span steel bridges are located on the interstate routes while the remaining bridges are equally distributed on the primary and secondary routes.

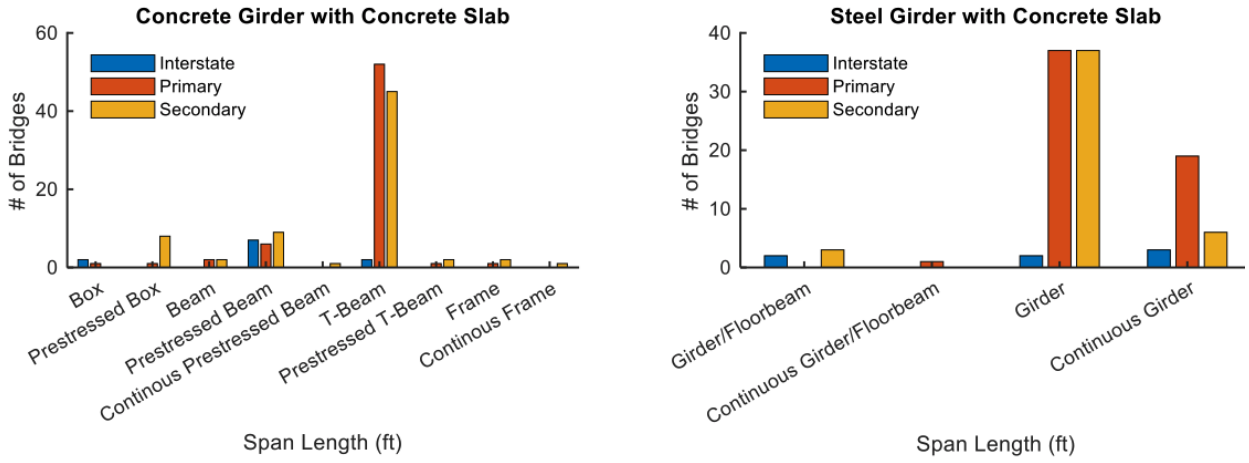

(a) **(b)**

Figure 8. Girder Bridges with RF < 1.0 Categorized Based on Superstructure Type: (a) concrete girder bridges; (b) steel girder bridges

Based on the above findings, three bridge classes were selected for the assessment of their load distribution behavior using refined analysis: (1) steel girder bridges; (2) reinforced concrete T-beam bridges; and (3) concrete slab bridges. For each of these bridge classes, the database of bridges with an RF < 1.0 was further analyzed to select representative bridges for each bridge class. In particular, the statistics of span length, number of lanes, and skew angle were analyzed for each bridge class. Although it was desirable to initially classify girder bridges also based on girder spacing and slab bridges based on slab thickness, this information was not available in the database.

Figures 9—11 show the distribution of steel girder bridges, concrete T-beam bridges, and slab bridges, respectively, based on span length, number of lanes, deck width, and skew angle. The summary of the statistical distributions is also provided in Tables 1—3. The average maximum span lengths for the steel girder, concrete T-beam, and slab bridges were 48.0 ft, 37.9 ft, and 20.0 ft, respectively. For the steel girder bridges, more than 90% of the bridges were non-skewed. For the concrete T-beam and slab bridges, most of the bridges were also non-skewed, but there were about 24% bridges with a skew angle of 30° or 45°. Two-lane bridges were the most common for all bridge classes and the average deck widths were about 28-29 ft.

Based on the above statistical distributions for each bridge class, population pools of 21, 25, and 25 bridges were selected for the refined analyses for the steel girder, concrete T-beam, and slab bridges, respectively. The selection was limited to 21-25 bridges due to the manual nature of the bridge plan acquisitions, structural detail extraction from those plans, and manual entry of relevant geometry required to develop the models. In the selection of bridges, a priority was also given to bridges located on interstate and primary routes. Additionally, some iteration

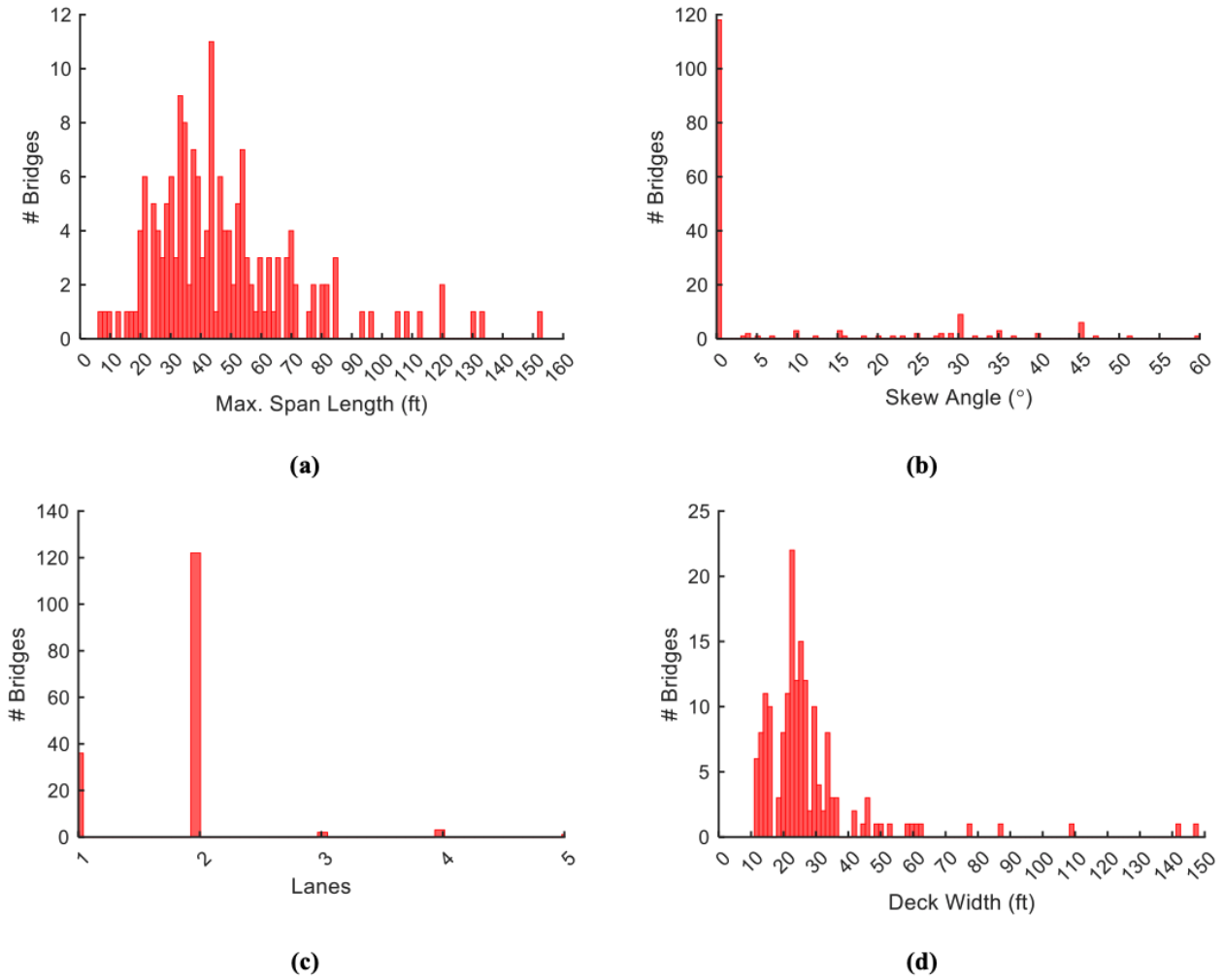

Figure 9. Steel Girder Bridges with a RF < 1.0, Categorized Based on: (a) span length; (b) number of lanes; (c) skew angle; (d) rating

on the selected pool was required because the details of the bridge geometries were only completely available after reviewing plans and the goal was to develop a pool that was geometrically representative of the population. Tables 4—6 provide the main properties of the selected bridges for the steel girder, concrete T-beam, and slab bridges, respectively.

Table 1. Statistical Parameters for Steel Girder Bridges with an RF < 1.0

Parameter	Minimum	Maximum	Average	Standard Deviation
Max Span (ft)	7	153	48	24.5
Skew (degrees)	0	60	8	14.5
Number of Lanes	1	9	2	1
Deck Width (ft)	12	148	28	18

Table 2. Statistical Parameters for Concrete T-Beam Bridges with an RF < 1.0

Parameter	Minimum	Maximum	Average	Standard Deviation
Max Span (ft)	15	56	37.9	7.2
Skew (degrees)	0	50	9	15.7
Number of Lanes	1	4	2	0.3
Deck Width (ft)	12	66	27.9	7.4

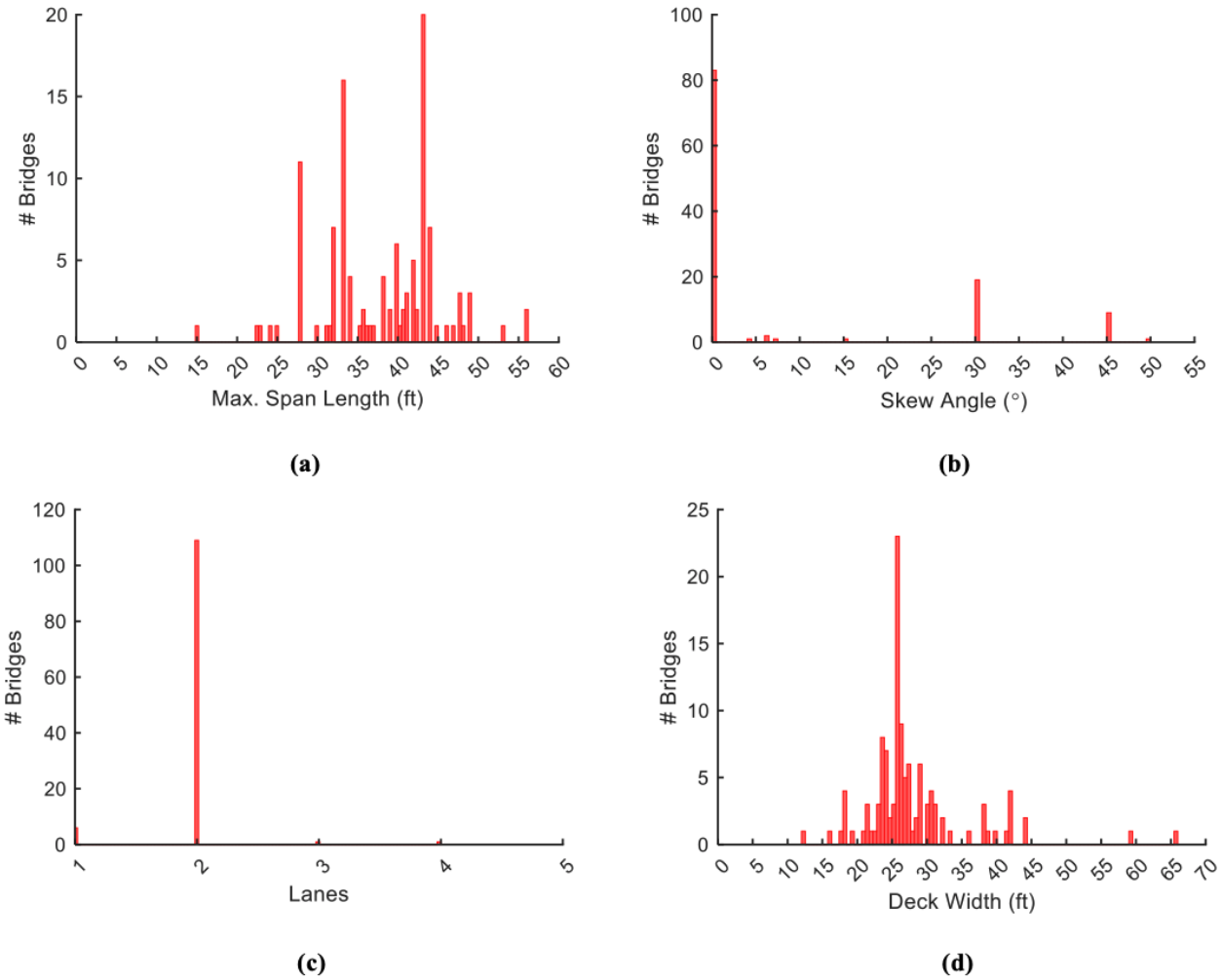

Figure 10. Concrete T-beam Bridges with a RF < 1.0 Categorized Based on: (a) span length; (b) skew angle; (c) number of lanes; (d) deck width

Table 3. Statistical Parameters for Concrete Slab Bridges with an RF < 1.0

Parameter	Minimum	Maximum	Average	Standard Deviation
Max Span (ft)	6	69	20	11
Skew (degrees)	0	45	12	17.6
Number of Lanes	1	5	2	0.52
Deck Width (ft)	11	101	29	11

Selection of Refined Analysis Method

Presented in this section is a brief synthesis of select results that were deemed suitable for validation of the modeling approaches with respect to measured field data from the studies. For the slab bridge, this included the grillage and 2D plate methods of analysis, while the beam bridge analyses utilized the eccentric beam and grillage methods of analysis. For the validation, the comparisons of model versus experimental results leveraged midspan bottom flange longitudinal strain for each of the girders for the steel girder bridge (S11) and T-beam bridge (Flat Creek), whereas longitudinal strain distributed transversely on the underside of the deck for

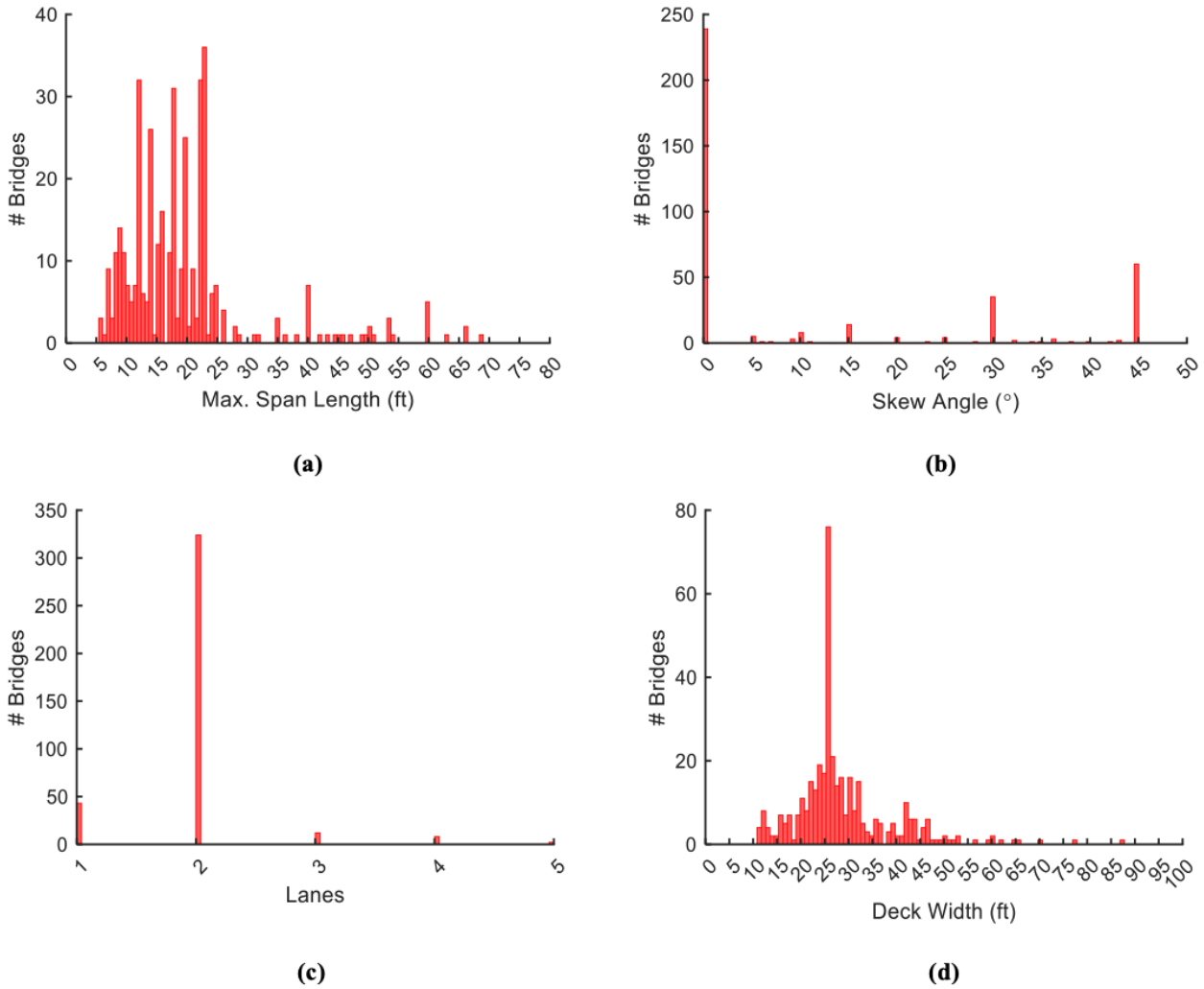

Figure 11. Concrete Slab Bridges with a RF < 1.0 Categorized Based on: (a) span length; (b) skew angle; (c) number of lanes; (d) deck width

the slab bridge (Smacks Creek). Results for these comparisons are illustrated in Figures 12—14. When comparing the results across all three bridges, the models were clearly able to describe the behavior characteristics with corresponding relative responses within the system.

For both the Flat Creek and Smacks Creek bridges, the eccentric beam and 2D plate formulations, respectively, agreed not only in behavior characteristics, but also magnitude of derived response with respect to experimental data. For the same structures, the grillage approach exhibited less agreement with respect to magnitude with apparent higher distributions within the system.

For the S11 bridge, in addition to field test results of the Eom and Nowak (2001) study, numerical results for the pin–roller scenario provided in the same study was also compared with the modelling approaches (grillage and eccentric beam) in the current study, without any attempt to calibrate the rotational restraint of the supports. This approach was adopted since the intent of

Table 4. Steel Girder Bridges Selected for Refined Analysis

No.	Bridge Key	Route	Span Length (ft)	Girder Spacing (ft)	Overall Section Depth (in)	Skew Angle (degrees)	Deck Width (ft)	Number of Lanes
1	10370	Primary	40.5	7.7	36.7	30	24.0	2
2	10711	Primary	92.5	8.3	44.6	0	26.0	2
3	11884	Primary	47.5	6.8	40.6	0	28.0	2
4	12165	Primary	61.0	10.0	71.3	0	42.7	3
5	12641	Primary	54.8	7.2	40.7	23	44.0	3
6	13273	Interstate	96.0	6.3	40.3	0	20.0	2
7	14852	Primary	83.8	9.0	44.1	37	56.0	4
8	18185	Primary	26.0	5.8	27.9	0	24.0	2
9	18928	Secondary	45.3	9.0	34.9	28	47.0	3
10	19596	Secondary	54.0	7.7	40.3	7	30.8	2
11	20201	Primary	72.5	6.5	42.9	79	39.0	2
12	20547	Primary	75.9	7.3	42.9	68	38.8	3
13	2432	Primary	42.5	7.5	36.8	45	24.0	2
14	24482	Primary	110.0	9.0	65.0	0	30.0	2
15	2621	Primary	55.0	6.8	40.3	0	27.8	2
16	356	Primary	32.5	7.7	34.4	0	26.0	2
17	4398	Primary	70.0	6.3	42.9	0	26.0	2
18	5792	Primary	85.0	6.8	44.9	0	34.8	2
19	7089	Interstate	106.5	7.9	65.0	0	66.6	5
20	7758	Primary	42.8	4.3	28.2	0	18.0	1
21	9371	Primary	70.9	6.6	43.4	0	28.0	2

the investigation was to judge performance of various methods for determining lateral load distribution instead of an exercise in model calibration. For this bridge, the grillage and eccentric beam formulations aligned better, but exhibited a departure from the experimental data. This departure is attributed to the effects of boundary conditions, which were shown from the Eom and Nowak (2001) study to exhibit a higher level of restraints than idealized models, thus resulting in lower (that is, more conservative) strain values than the idealized simple support models. Note that the results obtained from grillage and eccentric beam models of the current study aligned well with the numerical results obtained in Eom and Nowak (2001) study, where a pin-roller support assumption was also made.

Based on the results derived from these validations and other loading scenarios, the modeling approaches were both deemed suitable for continued study. While both sets of approaches (eccentric beam/grillage and 2D plate/grillage) proved effective, the eccentric beam and 2D plate analysis approaches provided an additional benefit due to model development efficiency within the LARSA 4D software package. Note that, for the eccentric beam analysis, LARSA 4D allows generating models automatically with little effort using built-in templates that can also be modified using spreadsheets. On the other hand, the grillage analysis in LARSA 4D requires additional efforts for the placement of grid lines and the calculations of some sectional properties, such as bending and torsional inertias. Therefore, the eccentric beam and 2D plate analysis approaches were used for the remainder of the study.

Table 5. Concrete T-beam Bridges Selected for Refined Analysis

No.	Bridge Key	Route	Span Length (ft)	Girder Spacing (ft)	Overall Section Depth (in)	Skew Angle (degrees)	Deck Width (ft)	Number of Lanes
1	1210	Primary	27.9	6.0	25.0	30	27.2	2
2	12384	Primary	34.1	9.6	35.6	30	31.0	2
3	12417	Primary	47.9	7.9	28.0	50	26.1	2
4	13184	Secondary	23.0	6.0	28.0	0	25.8	2
5	13867	Secondary	40.3	7.2	37.0	0	25.5	2
6	14023	Primary	40.0	6.0	36.3	0	36.8	2
7	15402	Secondary	40.0	9.0	36.4	0	20.4	2
8	15533	Secondary	40.0	7.2	39.0	0	27.9	2
9	16565	Primary	44.0	7.2	39.0	45	30.1	2
10	16566	Primary	44.0	7.2	39.0	45	26.2	2
11	1709	Primary	32.2	10.0	31.1	0	25.4	2
12	17237	Secondary	44.0	8.0	35.9	0	19.1	2
13	17757	Primary	32.0	9.0	31.4	0	22.5	2
14	18493	Primary	28.0	7.2	32.0	30	24.1	2
15	1892	Primary	26.0	6.0	25.0	30	28.3	2
16	2430	Primary	43.0	7.7	45.0	30	23.8	2
17	4357	Primary	24.9	5.1	32.1	0	23.8	4
18	4850	Primary	36.5	7.8	33.3	0	31.3	2
19	5100	Primary	45.9	7.6	39.6	45	27.1	2
20	7770	Primary	47.9	6.5	40.5	0	34.5	2
21	8022	Secondary	22.5	5.7	29.0	0	38.4	2
22	8690	Primary	42.5	7.2	26.8	0	26.0	2
23	912	Primary	43.0	7.6	41.9	45	30.8	2
24	9161	Primary	44.7	7.8	43.0	0	47.3	2
25	9317	Secondary	48.1	8.0	39.6	0	44.3	2

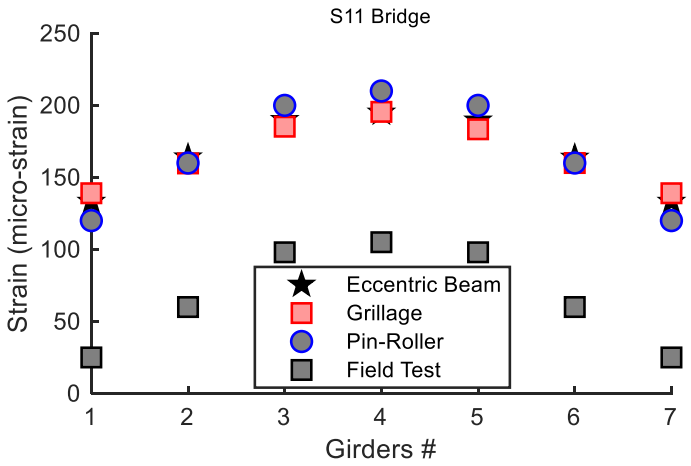

Figure 12. Model Validation for Steel Girder Bridge (S11 Bridge)

Table 6. Concrete Slab Bridges Selected for Refined Analysis

No.	Bridge Key	Route	Span Length (ft)	Skew Angle (degrees)	Deck Width (ft)	Section Depth (in)	Number of Lanes
1	391	Secondary	18.0	0	25.5	17.5	2
2	10588	Primary	20.0	0	25.5	19.0	2
3	21217	Primary	22.5	0	59.4	20.0	2
4	9107	Secondary	40.0	0	29.8	17.0	2
5	7855	Secondary	40.0	0	28.9	20.0	2
6	19539	Primary	22.0	10	36.0	18.5	2
7	3414	Secondary	15.1	5	25.9	15.0	2
8	3416	Secondary	14.1	15	25.9	14.0	2
9	26888	Secondary	54.0	15	28.0	20.0	2
10	2633	Primary	15.1	30	49.9	14.0	2
11	4361	Primary	20.0	30	77.1	19.0	2
12	18127	Secondary	40.0	30	26.9	20.0	2
13	5511	Secondary	17.1	35	22.0	17.5	4
14	3173	Primary	23.0	45	46.9	18.0	2
15	18900	Primary	20.0	45	28.0	15.0	2
16	13198	Primary	14.1	45	25.9	14.0	2
17	18840	Primary	23.0	0	25.5	22.0	4
18	13230	Primary	23.0	0	25.5	22.0	2
19	4545	Primary	23.0	0	25.5	19.5	2
20	10249	Primary	14.1	0	26.0	21.0	2
21	1870	Primary	14.1	0	25.5	21.0	2
22	18881	Primary	20.0	30	25.0	20.5	2
23	1185	Primary	24.0	30	26.3	16.0	2
24	17401	Primary	14.0	45	25.0	18.5	2
25	17694	Primary	23.0	45	17.5	17.5	2

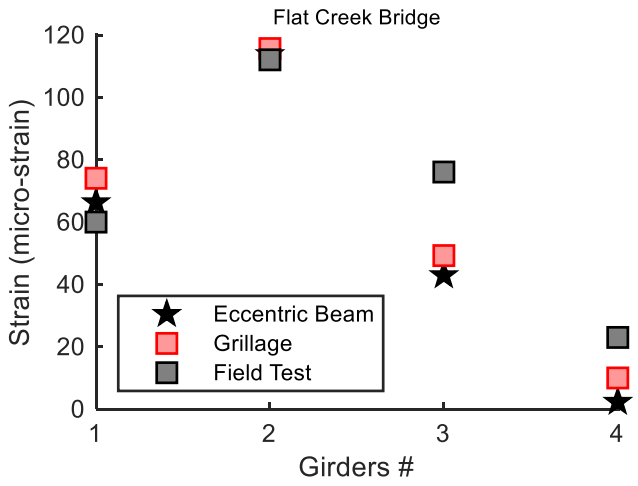

Figure 13. Model Validation for RC T-beam Bridge (Flat Creek Bridge)

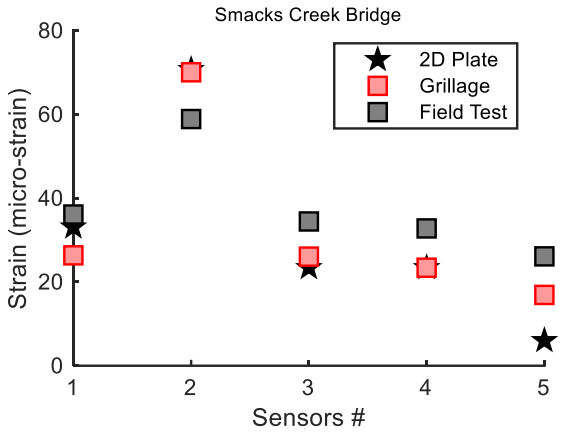

Figure 14. Model Validation for Concrete Slab Bridge (Smacks Creek Bridge)

Refined Analysis of Bridge Classes and Evaluation of Load Distribution Behavior

Results from Modeled Bridges

For the 21 steel girder bridges, 25 reinforced concrete T-beam bridges, and 25 reinforced concrete slab bridges, the relative performance of the refined methods of analyses are presented in Tables 7—9, respectively. As shown in each of these tables, the change in distribution factors (ΔDF) and load rating factors (ΔRF) are typically inversely proportional. Also, note that the change in effective width *(ΔEW)* is directly proportional to the load rating factor, i.e., an increase in the effective width will lead to an increased rating factor.

Prediction Models

A series of multi-parameter linear regression models were developed to predict the percent change in distribution factor for slab-on-girder bridges and percent change in effective width for slab bridges using four variables that described the geometrical characteristics of the bridges. Although all regression models use four variables, these variables differ in each model and were selected based on their significance in a given scenario. Also, note that the developed regression models and corresponding tables are reliable for the parameter space presented in each table. Each of the regressions models developed was validated through a comparison of the predictions to the results derived from the refined analyses.

The following notation applies to all of the prediction model equations and tables:

d = depth of beam or stringer (in.)
L = span of beam (ft)
N_b = number of beams, stringers, or girders
S = spacing of beams or webs (ft)
t_s = depth of concrete slab (in.)
W = edge-to-edge width of bridge (ft)
I = moment of inertia of beam (in^4)
θ = skew angle (degrees)

Table 7. Distribution and Load Rating Factors for Steel Girder Bridges – Refined Analyses Versus LRFD

Bridge No.	Interior Moment		Exterior Moment		Interior Shear		Exterior Shear	
	ΔDF	ΔRF	ΔDF	ΔRF	ΔDF	ΔRF	ΔDF	ΔRF
1	-6%	6%	0%	0%	6%	-6%	-5%	5%
2	-2%	2%	-11%	12%	9%	-8%	-2%	2%
3	-10%	11%	-50%	100%	13%	-12%	-53%	113%
4	-22%	28%	-33%	49%	31%	-24%	-12%	14%
5	-20%	25%	-22%	28%	8%	-7%	-21%	27%
6	0%	0%	0%	0%	0%	0%	6%	-6%
7	-14%	16%	7%	-7%	10%	-9%	-26%	35%
8	-17%	20%	-29%	41%	3%	-3%	-30%	43%
9	-18%	22%	-17%	20%	-4%	4%	-24%	32%
10	20%	-17%	-32%	47%	-14%	16%	-48%	92%
11	-37%	59%	-26%	35%	15%	-13%	-54%	117%
12	-19%	23%	-11%	12%	2%	-2%	-28%	39%
13	1%	-1%	-14%	16%	7%	-7%	-7%	8%
14	-2%	2%	-16%	19%	24%	-19%	-7%	8%
15	-7%	8%	-52%	108%	13%	-12%	-55%	122%
16	-2%	2%	-26%	35%	-2%	2%	-10%	11%
17	4%	-4%	-38%	61%	18%	-15%	-48%	92%
18	-12%	14%	24%	-19%	12%	-11%	81%	-45%
19	-31%	45%	-26%	35%	-7%	8%	10%	-9%
20	0%	0%	0%	0%	0%	0%	0%	0%
21	-4%	4%	-51%	104%	13%	-12%	-41%	69%

Table 8. Distribution and Load Rating Factors for T-Beam Bridges – Refined Analyses Versus LRFD

Bridge No.	Interior Moment		Exterior Moment		Interior Shear		Exterior Shear	
	ΔDF	ΔRF	ΔDF	ΔRF	ΔDF	ΔRF	ΔDF	ΔRF
1	6%	-6%	-43%	75%	4%	-4%	-25%	33%
2	-68%	213%	90%	-47%	-1%	1%	13%	-12%
3	15%	-13%	-18%	22%	-2%	2%	-34%	52%
4	20%	-17%	-42%	72%	26%	-21%	-33%	49%
5	-21%	27%	62%	-38%	12%	-11%	55%	-35%
6	-22%	28%	-14%	16%	9%	-8%	42%	-30%
7	3%	-3%	-15%	18%	44%	-31%	-12%	14%
8	3%	-3%	-18%	22%	26%	-21%	1%	-1%
9	22%	-18%	-3%	3%	20%	-17%	-7%	8%
10	12%	-11%	1%	-1%	7%	-7%	4%	-4%
11	0%	0%	-19%	23%	37%	-27%	-2%	2%
12	18%	-15%	-19%	23%	0%	0%	0%	0%
13	-4%	4%	-18%	22%	43%	-30%	-9%	10%
14	10%	-9%	-16%	19%	26%	-21%	-15%	18%
15	-11%	12%	-8%	9%	-3%	3%	-30%	43%
16	1%	-1%	13%	-12%	7%	-7%	40%	-29%
17	-12%	14%	0%	0%	11%	-10%	24%	-19%
18	-11%	12%	-9%	10%	22%	-18%	-4%	4%
19	8%	-7%	8%	-7%	21%	-17%	6%	-6%
20	-8%	9%	-1%	1%	4%	-4%	25%	-20%
21	-38%	61%	76%	-43%	20%	-17%	17%	-15%
22	5%	-5%	3%	-3%	25%	-20%	1%	-1%
23	10%	-9%	16%	-14%	14%	-12%	57%	-36%
24	-25%	33%	-27%	37%	-7%	8%	10%	-9%
25	-27%	37%	-34%	52%	17%	-15%	-9%	10%

Table 1. Effective Width for Slab Bridges – Refined Analyses versus LRFD

Bridge No.	ΔEW - Single Lane	ΔEW - Multi-lane
1	81%	6%
2	44%	5%
3	26%	-6%
4	-14%	-10%
5	4%	3%
6	61%	22%
7	68%	13%
8	80%	11%
9	2%	-8%
10	57%	17%
11	71%	38%
12	4%	1%
13	24%	0%
14	37%	24%
15	32%	12%
16	9%	2%
17	56%	5%
18	25%	3%
19	25%	3%
20	67%	5%
21	66%	9%
22	24%	7%
23	23%	2%
24	14%	6%
25	34%	0%

Ov = overhang length (ft)
DF = distribution factor
P_w = parapet width (ft)
ΔDF = percent change in distribution factor
ΔE_w = percent change in effective width

Steel Girder Bridges

Interior Moment. The regression model developed for interior moment is shown in Equation (7). This four-parameter model had an R^2 value of 0.715. The primary parameters associated with this were number of girders, girder depth, girder spacing, and skew. Tables 10 and 11 illustrate the impacts across the parameter space for both distribution factor and load rating factor. Recall that the distribution and rating factors are inversely correlated, where a reduction in the distribution factor corresponds to an increase in the rating factor. Thus, subsequent discussions will focus on the change in the distribution factors.

$$\Delta DF_{int\text{-}M} = -21 + 0.8S - 5.7N_b + 1.21\theta + 2.40d + 1.03S \cdot N_b + 0.066S \cdot \theta - 0.202S \cdot d - 0.193N_b \cdot \theta - 0.168N_b \cdot d + 0.0501\theta \cdot d \quad (7)$$

Observations from these results include: As the number of girders increased, the greater the possibility of reducing the distribution factor.

Table 10. Percent Change in Distribution Factors for Interior Moment for Steel Girder Bridges

	d =	25				30				35				40				45			
	N_b =	4	5	6	7	4	5	6	7	4	5	6	7	4	5	6	7	4	5	6	7
θ=0	S=6	-1	-5	-9	-13	1	-3	-8	-12	4	-2	-7	-12	6	0	-6	-12	9	2	-5	-12
	S=7	-2	-4	-7	-10	0	-3	-7	-11	2	-3	-7	-11	3	-2	-7	-12	5	-1	-7	-13
	S=8	-2	-3	-5	-7	-1	-4	-6	-9	-1	-4	-7	-11	0	-4	-8	-13	1	-4	-9	-14
	S=9	-2	-2	-3	-4	-2	-4	-5	-7	-3	-5	-7	-10	-3	-6	-9	-13	-4	-8	-12	-16
θ=15	S=6	-6	-13	-20	-26	0	-8	-15	-22	6	-2	-10	-19	13	3	-6	-15	19	9	-1	-11
	S=7	-6	-11	-17	-22	0	-7	-13	-19	5	-2	-9	-17	10	2	-6	-14	16	7	-2	-11
	S=8	-5	-9	-14	-18	0	-6	-11	-17	4	-2	-8	-15	8	1	-6	-13	13	5	-3	-11
	S=9	-4	-7	-11	-14	0	-5	-9	-14	3	-2	-8	-13	6	0	-6	-12	9	3	-4	-11
θ=30	S=6	-11	-21	-30	-40	-1	-12	-22	-32	9	-2	-14	-25	19	7	-5	-17	29	16	3	-10
	S=7	-10	-18	-26	-35	0	-10	-19	-28	9	-2	-12	-22	18	7	-4	-15	27	15	3	-9
	S=8	-8	-15	-23	-30	0	-8	-16	-24	8	-1	-10	-19	17	7	-3	-13	25	14	3	-8
	S=9	-6	-12	-19	-25	1	-6	-13	-21	8	0	-8	-16	15	6	-3	-11	22	13	3	-7
θ=45	S=6	-16	-29	-41	-54	-3	-16	-29	-42	11	-3	-17	-31	25	10	-5	-20	39	23	7	-8
	S=7	-14	-25	-36	-48	-1	-13	-25	-37	12	-1	-14	-27	25	11	-3	-17	38	23	8	-6
	S=8	-11	-21	-31	-42	1	-10	-21	-32	13	1	-11	-23	25	12	-1	-14	37	23	9	-4
	S=9	-8	-17	-26	-36	3	-7	-17	-28	14	3	-8	-19	25	13	1	-11	35	23	10	-3

θ = skew in the bridge, in degrees; S = girder spacing, in feet; d = girder depth, in inches; N_b = number of girders

Table 11. Percent Change in Rating Factors for Interior Moment for Steel Girder Bridges

	d =	25				30				35				40				45			
	N_b =	4	5	6	7	4	5	6	7	4	5	6	7	4	5	6	7	4	5	6	7
θ=0	S=6	1	5	10	14	-1	3	9	14	-4	2	8	14	-6	0	7	14	-8	-2	6	14
	S=7	2	4	7	11	0	4	8	12	-2	3	8	13	-3	2	8	14	-5	1	8	15
	S=8	2	3	5	7	1	4	6	9	1	4	8	12	0	4	9	14	-1	5	10	17
	S=9	2	2	3	4	2	4	5	7	3	5	8	11	3	7	10	14	4	8	13	18
θ=15	S=6	7	15	24	36	0	8	18	29	-6	2	11	23	-11	-3	6	17	-16	-8	1	12
	S=7	6	12	20	29	0	7	15	24	-5	2	10	20	-9	-2	6	16	-14	-6	2	12
	S=8	5	10	16	22	0	6	13	20	-4	2	9	17	-8	-1	6	15	-11	-4	3	13
	S=9	4	8	12	17	0	5	10	16	-3	2	8	15	-6	0	6	14	-9	-2	5	13
θ=30	S=6	13	26	44	66	1	13	28	48	-8	2	16	33	-16	-6	5	21	-22	-14	-3	11
	S=7	11	22	36	54	0	11	24	40	-8	2	13	28	-15	-6	4	18	-21	-13	-3	10
	S=8	8	18	29	43	0	9	19	32	-8	1	11	23	-14	-6	4	15	-20	-12	-3	8
	S=9	6	14	23	34	-1	6	15	26	-8	0	9	19	-13	-6	3	13	-18	-11	-3	7
θ=45	S=6	20	40	70	116	3	19	41	73	-10	3	20	45	-20	-9	5	24	-28	-19	-7	9
	S=7	16	33	57	91	1	15	34	60	-11	1	16	37	-20	-10	3	20	-27	-19	-8	7
	S=8	12	27	46	72	-1	11	27	48	-11	-1	12	30	-20	-11	1	16	-27	-19	-8	5
	S=9	9	21	36	56	-3	8	21	38	-12	-3	9	24	-20	-11	-1	12	-26	-19	-9	3

θ = skew in the bridge, in degrees; S = girder spacing, in feet; d = girder depth, in inches; N_b = number of girders

- Bridges with high skew angles had a higher chance of experiencing a reduction in distribution factor when a refined analysis was conducted. For highly skewed bridges, the
- largest reduction was associated with bridges that had a small girder depth and higher number of girders.
- As the girder depth increased, there was a lower probability of a reduction in the distribution factor. For the bridges with a high girder depth and small number of girders, even a small increase in the distribution factors can be observed.
- Girder spacing had minimal effect on the change in distribution factors.

Exterior Moment. The regression model developed for exterior moment is shown in Equation (8). This four-parameter model has an R^2 value of 0.858. The primary parameters associated with this model are girder depth, span length, skew angle, and slab thickness. Tables 12 and 13 illustrate the impacts across the parameter space for the distribution factor and load rating factor, respectively.

$$\Delta DF_{ext\text{-}M} = 358 + 2.43L - 51.4t_s - 18.13d - 2.19\theta - 0.018L{\cdot}t_s - 0.0391L{\cdot}d \\ -0.0280L{\cdot}\theta + 2.161t_s.d + 0.098t_s \cdot \theta + 0.109d \cdot \theta \quad (8)$$

Observations from these results include:

- As the slab thickness decreased, the distribution factors tended to be larger relative to the AASHTO-calculated factors.

Table 12. Percent Change in Distribution Factors for Exterior Moment for Steel Girder Bridges

	d =	25			30			35			40			45		
	t_s =	7	8	9	7	8	9	7	8	9	7	8	9	7	8	9
θ=0	L=45	-29	-16	-3	-37	-24	-10	-44	-31	-18	-52	-39	-26	-59	-46	-33
	L=55	-24	-11	3	-31	-18	-5	-39	-26	-13	-47	-33	-20	-54	-41	-27
	L=65	-18	-5	8	-26	-13	0	-34	-20	-7	-41	-28	-15	-48	-35	-22
	L=75	-13	0	13	-21	-7	6	-28	-15	-2	-36	-23	-9	-43	-30	-17
	L=85	-8	6	19	-15	-2	11	-23	-10	4	-31	-17	-4	-38	-24	-11
θ=15	L=45	-26	-13	1	-34	-20	-7	-41	-28	-15	-49	-36	-22	-56	-43	-29
	L=55	-21	-7	6	-28	-15	-2	-36	-23	-9	-43	-30	-17	-51	-37	-24
	L=65	-15	-2	11	-23	-10	4	-30	-17	-4	-38	-25	-12	-45	-32	-19
	L=75	-10	3	17	-17	-4	9	-25	-12	1	-33	-19	-6	-40	-27	-13
	L=85	-4	9	22	-12	1	14	-20	-6	7	-27	-14	-1	-34	-21	-8
θ=30	L=45	-23	-9	4	-30	-17	-4	-38	-25	-11	-46	-32	-19	-53	-39	-26
	L=55	-17	-4	9	-25	-12	2	-33	-19	-6	-40	-27	-14	-47	-34	-21
	L=65	-12	1	15	-20	-6	7	-27	-14	-1	-35	-22	-8	-42	-29	-15
	L=75	-7	7	20	-14	-1	12	-22	-9	5	-29	-16	-3	-37	-23	-10
	L=85	-1	12	25	-9	4	18	-16	-3	10	-24	-11	2	-31	-18	-5
θ=45	L=45	-19	-6	7	-27	-14	-1	-35	-21	-8	-42	-29	-16	-49	-36	-23
	L=55	-14	-1	12	-22	-8	5	-29	-16	-3	-37	-24	-10	-44	-31	-18
	L=65	-9	5	18	-16	-3	10	-24	-11	3	-32	-18	-5	-39	-25	-12
	L=75	-3	10	23	-11	2	16	-19	-5	8	-26	-13	0	-33	-20	-7
	L=85	2	15	29	-6	8	21	-13	0	13	-21	-8	6	-28	-15	-1

θ = skew in the bridge, in degrees; L = span length, in feet; d = beam depth, in inches; t_s = slab thickness, in inches

Table 13. Percent Change in Rating Factors for Exterior Moment for Steel Girder Bridges

d =		25			30			35			40			45		
t_s =		7	8	9	7	8	9	7	8	9	7	8	9	7	8	9
θ=0	L=45	41	19	3	58	31	11	80	45	22	109	63	34	145	85	48
	L=55	31	12	-3	46	22	5	64	35	14	88	50	25	116	68	38
	L=65	23	5	-7	35	15	0	51	26	8	70	39	17	94	54	28
	L=75	15	0	-12	26	8	-5	40	18	2	56	29	10	76	42	20
	L=85	8	-5	-16	18	2	-10	30	11	-3	44	21	4	60	32	13
θ=15	L=45	35	15	-1	51	25	8	70	39	17	95	55	29	127	74	42
	L=55	26	8	-6	39	18	2	56	29	10	77	43	20	102	59	32
	L=65	18	2	-10	30	11	-4	44	21	4	62	33	13	82	47	23
	L=75	11	-3	-14	21	4	-8	33	13	-1	49	24	7	66	36	15
	L=85	5	-8	-18	14	-1	-13	25	7	-6	38	16	1	53	27	9
θ=30	L=45	29	10	-4	44	21	4	61	33	13	84	48	24	111	65	35
	L=55	21	4	-8	33	13	-2	48	24	6	67	37	16	90	52	26
	L=65	14	-1	-13	24	7	-6	37	16	1	53	28	9	72	40	18
	L=75	7	-6	-17	17	1	-11	28	9	-4	42	19	3	58	30	11
	L=85	1	-11	-20	10	-4	-15	20	3	-9	32	12	-2	45	22	5
θ=45	L=45	24	7	-7	37	16	1	53	27	9	73	41	19	98	57	30
	L=55	16	1	-11	28	9	-5	42	19	3	59	31	12	79	45	21
	L=65	10	-4	-15	20	3	-9	32	12	-2	46	22	5	63	34	14
	L=75	3	-9	-19	12	-2	-13	23	6	-7	36	15	0	50	25	7
	L=85	-2	-13	-22	6	-7	-17	15	0	-12	26	8	-5	39	17	1

θ = skew in the bridge, in degrees; L = span length, in feet; d = beam depth, in inches; t_s = slab thickness, in inches

- An increase in span length resulted in a decrease in potential reduction in distribution factor.
- As the skew angle increased, the possibility of reduction in distribution factors somewhat decreased.
- Bridges with higher girder depth have a larger chance of experiencing a reduction in distribution factor.

Interior Shear. The regression model developed for interior shear is shown in Equation (9). This four-parameter model has an R^2 value of 0.742. The primary parameters associated with this model are girder depth, overhang length, skew angle, and number of girders. Tables 14 and 15 illustrate the impacts across the parameter space for the distribution and load rating factors, respectively. Observations from these results include:

- Distribution factors mostly increased for bridges with characteristics that are within the bounds given in Table 14. In other words, the rating factor for bridges could be expected to decrease when using refined analysis methods and the rating is controlled by shear capacity of interior beams.
- An increase in girder depth typically lead to an increase in distribution factor.
- Bridges with a high skew angle (30 or 45 degrees) and small girder depth tended to have a reduction in the distribution factor. The magnitude of this reduction increased with an increasing number of girders.

$$\Delta DF_{int\text{-}S} = -109.5 + 2.11d + 87.8O_v - 0.690\theta + 14.1N_b - 0.969d \cdot O_v + 0.0677d \cdot \theta - 0.208d \cdot N_b - 0.497O_v \cdot \theta - 6.2O_v \cdot N_b - 0.244\theta \cdot N_b \quad (9)$$

Table 14. Percent Change in Distribution Factors for Interior Shear for Steel Girder Bridges

	N_b =	4			5			6			7			8		
	Ov =	0.4	0.8	0.12	0.4	0.8	0.12	0.4	0.8	0.12	0.4	0.8	0.12	0.4	0.8	0.12
θ=0	d=25	-6	10	25	1	14	27	7	18	28	14	22	30	20	26	31
	d=30	-1	12	26	4	15	26	10	18	27	15	21	27	20	24	28
	d=35	3	15	27	8	17	26	12	19	25	16	20	25	21	22	24
	d=40	8	17	27	11	18	25	14	19	24	18	20	22	21	21	20
	d=45	12	20	28	14	20	25	17	19	22	19	19	20	21	19	17
θ=15	d=25	-8	4	17	-5	5	15	-3	5	12	0	5	10	3	5	8
	d=30	1	12	22	3	11	19	5	10	16	6	10	13	8	9	10
	d=35	11	19	28	12	18	24	12	16	20	13	14	15	14	12	11
	d=40	20	27	34	20	24	28	20	21	23	19	19	18	19	16	13
	d=45	30	35	39	28	31	33	27	27	27	26	23	20	24	19	14
θ=30	d=25	-11	-1	8	-12	-5	2	-13	-8	-3	-14	-11	-9	-14	-15	-15
	d=30	4	11	19	2	7	12	0	3	5	-2	-2	-2	-4	-6	-9
	d=35	18	24	30	15	19	22	12	13	14	9	8	6	6	2	-2
	d=40	33	37	40	29	30	31	25	24	23	21	17	14	17	11	5
	d=45	48	49	51	43	42	41	37	34	31	32	27	21	27	19	11
θ=45	d=25	-13	-7	0	-18	-14	-10	-23	-21	-19	-27	-28	-29	-32	-35	-38
	d=30	6	11	16	1	3	5	-5	-5	-6	-11	-13	-16	-16	-21	-27
	d=35	26	29	31	19	20	20	13	10	8	6	1	-3	-1	-8	-15
	d=40	46	46	47	38	36	35	30	26	22	23	16	9	15	6	-3
	d=45	65	64	63	57	53	49	48	42	36	39	31	22	30	19	8

θ = skew in the bridge, in degrees; d = beam depth, in inches; N_b = number of girders; Ov = overhang, in feet

Table 15. Percent Change in Rating Factors for Interior Shear for Steel Girder Bridges

	N_b =	4			5			6			7			8		
	Ov =	0.4	0.8	0.12	0.4	0.8	0.12	0.4	0.8	0.12	0.4	0.8	0.12	0.4	0.8	0.12
θ=0	d=25	6	-9	-20	-1	-12	-21	-7	-15	-22	-12	-18	-23	-17	-20	-24
	d=30	1	-11	-21	-4	-13	-21	-9	-15	-21	-13	-17	-21	-17	-19	-22
	d=35	-3	-13	-21	-7	-14	-21	-11	-16	-20	-14	-17	-20	-17	-18	-19
	d=40	-7	-15	-21	-10	-15	-20	-13	-16	-19	-15	-17	-18	-17	-17	-17
	d=45	-11	-17	-22	-13	-16	-20	-14	-16	-18	-16	-16	-16	-17	-16	-14
θ=15	d=25	9	-4	-14	6	-4	-13	3	-5	-11	0	-5	-9	-3	-5	-7
	d=30	-1	-11	-18	-3	-10	-16	-5	-9	-14	-6	-9	-11	-8	-8	-9
	d=35	-10	-16	-22	-10	-15	-19	-11	-14	-16	-11	-12	-13	-12	-11	-10
	d=40	-17	-21	-25	-17	-20	-22	-16	-18	-19	-16	-16	-15	-16	-14	-11
	d=45	-23	-26	-28	-22	-24	-25	-21	-21	-21	-20	-19	-17	-20	-16	-12
θ=30	d=25	12	1	-8	13	5	-2	14	9	4	16	13	10	17	17	18
	d=30	-4	-10	-16	-2	-7	-11	0	-3	-5	2	2	2	4	7	9
	d=35	-16	-19	-23	-13	-16	-18	-11	-12	-12	-9	-7	-6	-6	-2	2
	d=40	-25	-27	-29	-22	-23	-24	-20	-19	-18	-17	-15	-12	-14	-10	-4
	d=45	-32	-33	-34	-30	-30	-29	-27	-26	-24	-24	-21	-17	-21	-16	-10
θ=45	d=25	15	7	0	22	16	11	29	26	24	37	39	40	46	54	62
	d=30	-6	-10	-13	-1	-3	-5	5	6	6	12	15	19	19	27	36
	d=35	-21	-22	-24	-16	-16	-16	-11	-9	-8	-6	-1	4	1	8	18
	d=40	-31	-32	-32	-28	-27	-26	-23	-21	-18	-18	-14	-8	-13	-5	4
	d=45	-40	-39	-39	-36	-35	-33	-32	-29	-26	-28	-23	-18	-23	-16	-8

θ = skew in the bridge, in degrees; d = beam depth, in inches; N_b = number of girders; Ov = overhang, in feet

Exterior Shear. The regression model developed for exterior shear is shown in Equation (10). This four-parameter model has an R^2 value of 0.894. The primary parameters associated with this model are moment of inertia, slab thickness, span length, and girder spacing. Tables 16 and 17 illustrate the impacts across the parameter space for both distribution factor and load rating factor. Observations from these results include:

- As the slab thickness increased, the distribution factors tended to have a lower probability of a reduction.
- For bridges with slab thickness of 7 inches, the largest reductions in distribution factors occurred for bridges with short span lengths and high girder moments of inertia.
- For bridges with a slab thickness greater than 7 inches, the distribution factors increased as the span length increased and the girder spacing decreased.

$$\Delta DF_{ext\text{-}S} = -1424 + 2.35L + 197.4S + 186.7t_s - 0.0514I - 0.256L \cdot S + 0.085\, L \cdot t_s - 26.3S \cdot t_s + 0.0016S \cdot I + 0.0041t_s \cdot I \quad (10)$$

Table 16. Percent Change in Distribution Factors for Exterior Shear for Steel Girder Bridges

	t_s =	7			8			9		
	S =	6	7	8	6	7	8	6	7	8
I=4500	L=45	-33	-24	-15	18	1	-16	70	26	-18
	L=55	-19	-12	-6	33	13	-6	85	39	-7
	L=65	-5	-1	3	48	26	3	101	52	4
	L=75	9	11	12	63	38	13	117	66	14
	L=85	24	22	21	78	51	23	133	79	25
I=5500	L=45	-46	-35	-25	9	-6	-22	65	23	-19
	L=55	-32	-24	-16	24	6	-12	80	36	-9
	L=65	-18	-12	-7	39	18	-2	96	49	2
	L=75	-4	-1	2	54	31	7	112	62	13
	L=85	10	11	11	69	43	17	128	76	23
I=6500	L=45	-59	-47	-35	0	-14	-28	60	19	-21
	L=55	-45	-35	-26	15	-1	-18	75	33	-10
	L=65	-31	-24	-17	30	11	-8	91	46	0
	L=75	-17	-12	-8	45	23	2	107	59	11
	L=85	-3	-1	1	60	36	11	123	72	22
I=7500	L=45	-72	-58	-45	-9	-21	-34	55	16	-23
	L=55	-58	-47	-36	6	-9	-24	71	29	-12
	L=65	-44	-35	-27	21	4	-14	86	42	-1
	L=75	-30	-24	-18	36	16	-4	102	56	9
	L=85	-16	-12	-9	51	28	6	118	69	20
I=8500	L=45	-85	-70	-54	-18	-29	-40	50	13	-25
	L=55	-71	-58	-46	-3	-16	-30	66	26	-14
	L=65	-57	-47	-37	12	-4	-20	81	39	-3
	L=75	-43	-35	-28	27	9	-10	97	52	7
	L=85	-29	-24	-19	42	21	0	113	66	18

I = girder moment of inertia, in inches^4; L = span length, in feet; t_s = slab thickness, in inches; S = girder spacing, in feet

Table 17. Percent Change in Rating Factors for Exterior Shear for Steel Girder Bridges

	t_s =	7			8			9		
	S =	6	7	8	6	7	8	6	7	8
I=4500	L=45	-33	-24	-15	18	1	-16	70	26	-18
	L=55	-19	-12	-6	33	13	-6	85	39	-7
	L=65	-5	-1	3	48	26	3	101	52	4
	L=75	9	11	12	63	38	13	117	66	14
	L=85	24	22	21	78	51	23	133	79	25
I=5500	L=45	-46	-35	-25	9	-6	-22	65	23	-19
	L=55	-32	-24	-16	24	6	-12	80	36	-9
	L=65	-18	-12	-7	39	18	-2	96	49	2
	L=75	-4	-1	2	54	31	7	112	62	13
	L=85	10	11	11	69	43	17	128	76	23
I=6500	L=45	-59	-47	-35	0	-14	-28	60	19	-21
	L=55	-45	-35	-26	15	-1	-18	75	33	-10
	L=65	-31	-24	-17	30	11	-8	91	46	0
	L=75	-17	-12	-8	45	23	2	107	59	11
	L=85	-3	-1	1	60	36	11	123	72	22
I=7500	L=45	-72	-58	-45	-9	-21	-34	55	16	-23
	L=55	-58	-47	-36	6	-9	-24	71	29	-12
	L=65	-44	-35	-27	21	4	-14	86	42	-1
	L=75	-30	-24	-18	36	16	-4	102	56	9
	L=85	-16	-12	-9	51	28	6	118	69	20
I=8500	L=45	-85	-70	-54	-18	-29	-40	50	13	-25
	L=55	-71	-58	-46	-3	-16	-30	66	26	-14
	L=65	-57	-47	-37	12	-4	-20	81	39	-3
	L=75	-43	-35	-28	27	9	-10	97	52	7
	L=85	-29	-24	-19	42	21	0	113	66	18

I = girder moment of inertia, in inches^4; L = span length, in feet; t_s = slab thickness, in inches; S = girder spacing, in feet

Model Validation. The regression models were validated through a comparison of the predictions from the regression models to the results derived directly from the refined analyses of each bridge. The change in the distribution factor for the moment and shear obtained from either refined analysis (x-axis) or regression model (y-axis) are shown in Figure 15 for each steel girder bridge. The solid line in the plots indicates no difference between these two parameters. The dashed lines in the plots represent the limits of 10% error between the regression model and the refined analysis model. Note that the regression models are intended to be used within the boundaries set for the parameters shown in Tables 10 through 17. However, in the plots below, the models were also used to predict the percent change in the distribution factor for a bridge that is outside the parameter ranges of the model. These predictions are shown with a square red marker in the plots with the corresponding bridge number. The results indicated that the prediction model developed herein made a reasonable estimate for the majority of the bridges used in this study. However, as bridges approached or extended beyond the parameter space, the models tended to lose accuracy, which was expected. For example, the regression model did not provide a good estimate for Bridge 14 for the percent change in the distribution factor for interior moment, as can be seen from Figure 15 (a). However, Bridge 14 had a span length of 110 ft that

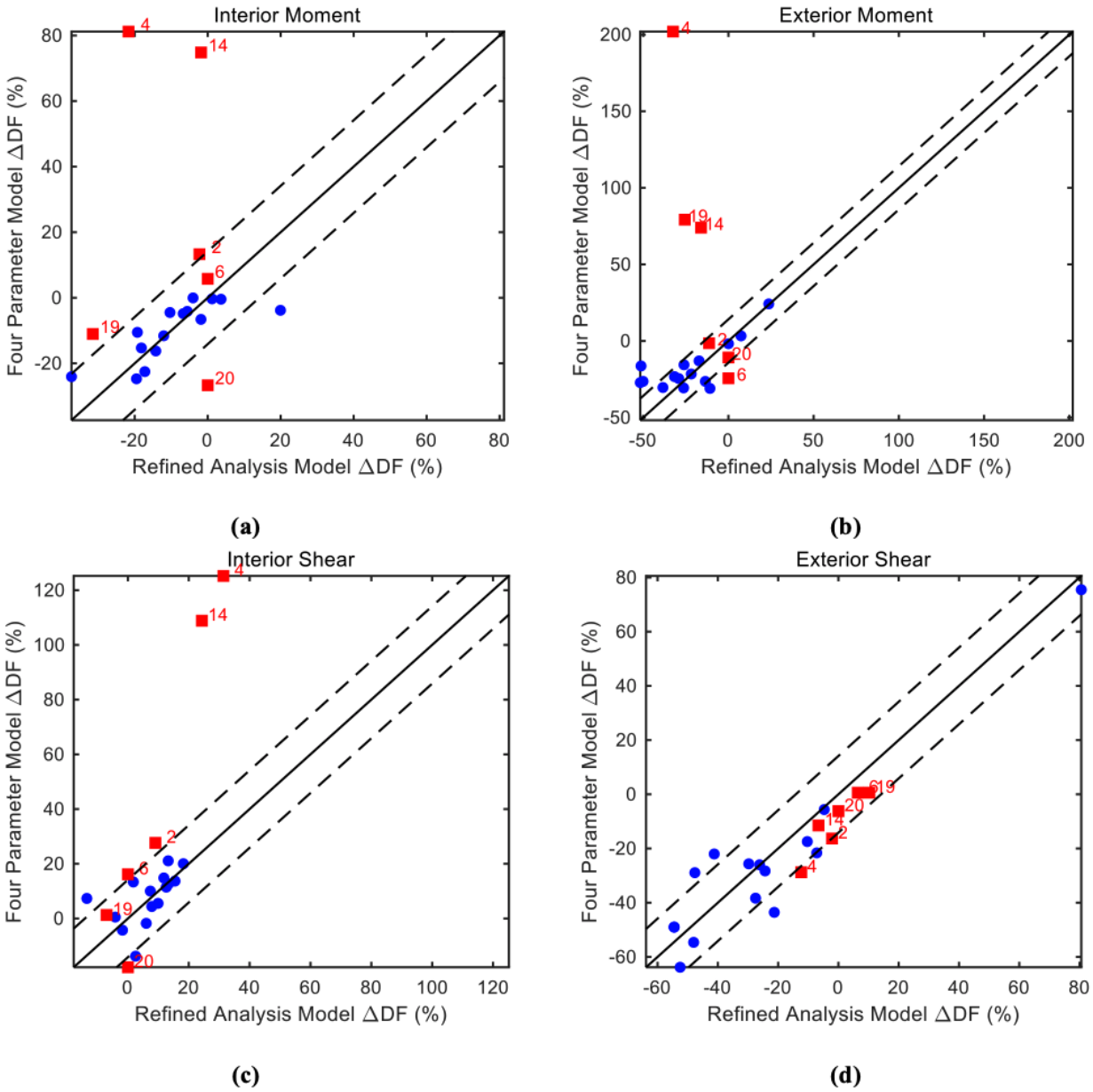

Figure 15. Percent Change in Distribution Factor for Steel Girder Bridges - Refined Analysis Versus Regression Model: (a) interior moment; (b) exterior moment; (c) interior shear; (d) exterior shear. Blue markers represent bridges within the parameter ranges of the regression model, while red markers represent bridges outside that parameter range together with corresponding bridge numbers from Table 4.

was well outside the 85-ft maximum span in the regression model. Similar boundary infringements existed for Bridges 2, 4, 10, 19, and 20.

Reinforced Concrete T-Beam Bridges

Interior Moment. The regression model developed for interior moment is shown in Equation (11). This four-parameter model has an R^2 value of 0.7131 (71.31%). The primary parameters associated with this model were number of girders, girder depth, girder spacing, and

span length. Tables 18 and 19 illustrate the impacts across the parameter space for both distribution factor and load rating factor. Observations from these results include:

- As the number of girders increased, the greater the possibility of reducing the distribution factor. For bridges with a small number of girders, the distribution factor mostly increased.
- An increase in girder spacing lead to a higher probability of reduction in the distribution factor.
- Bridges with a shorter span length and a higher number of girders had the highest possibility of experiencing a reduction in the distribution factor.
- Girder depth had minimal effect on the change in distribution factors.

$$\Delta DF_{int\text{-}M} = 387.36 - 12.66L + 11.40S - 4.536d - 32.59N_b + 0.93L \cdot S - 1.95S \cdot d + 1.05d \cdot N_b + 0.33L \cdot d - 0.3L \cdot N_b - 0.79S \cdot N_b \quad (11)$$

Table 18. Percent Change in Distribution Factors for Interior Moment for T-Beam Bridges

	d =	24				26				28				30			
	N_b =	3	4	5	6	3	4	5	6	3	4	5	6	3	4	5	6
L=34	**S=6**	28	6	-16	-39	25	4	-16	-36	21	3	-15	-33	17	1	-15	-31
	S=7	22	-1	-24	-47	15	-6	-27	-48	7	-12	-31	-50	0	-17	-34	-51
	S=8	16	-8	-32	-55	5	-17	-39	-61	-7	-26	-46	-66	-18	-36	-53	-71
L=36	**S=6**	28	5	-18	-41	26	5	-16	-37	24	5	-14	-33	21	5	-12	-29
	S=7	24	0	-23	-47	18	-4	-25	-47	12	-8	-27	-47	5	-12	-30	-47
	S=8	20	-5	-29	-54	10	-13	-35	-57	0	-21	-41	-61	-11	-29	-47	-65
L=38	**S=6**	28	5	-19	-43	27	6	-16	-37	26	7	-13	-32	25	8	-9	-27
	S=7	26	1	-23	-47	21	-1	-24	-46	16	-4	-24	-44	11	-7	-25	-43
	S=8	23	-2	-27	-52	15	-8	-31	-54	6	-15	-36	-57	-3	-22	-41	-59
L=40	**S=6**	28	4	-20	-45	28	6	-16	-38	29	9	-11	-31	29	11	-7	-25
	S=7	28	3	-22	-47	24	1	-22	-45	20	0	-21	-42	17	-2	-21	-39
	S=8	27	1	-24	-50	20	-4	-28	-51	12	-9	-31	-53	5	-15	-34	-54
L=42	**S=6**	28	3	-22	-46	29	7	-16	-39	31	10	-10	-31	33	14	-4	-23
	S=7	29	4	-22	-47	27	3	-20	-43	25	3	-18	-39	22	3	-16	-35
	S=8	31	4	-22	-48	24	0	-24	-48	18	-4	-26	-48	12	-8	-28	-48

L = span length, in feet; S = girder spacing, in feet; d = beam depth, in inches; N_b = number of girders

Exterior Moment. The regression model developed for exterior moment is shown in Equation (12). This four-parameter model had an R^2 value of 0.7875 (78.75%). The primary parameters associated with this model were number of girders, span length, girder spacing, and slab thickness. Tables 20 and 21 illustrate the impacts across the parameter space for both distribution factor and load rating factor.

$$\Delta DF_{ext\text{-}M} = -9771.88 + 182.9712L + 855.1251S + 1444.5060t_s - 16.5419L \cdot S - 27.0902L \cdot t_s + 3.6424L \cdot N_b - 159.4437S \cdot t_s + 127.1958S \cdot N_b + 3.1662L \cdot S \cdot t_s - 2.7733L \cdot S \cdot N_b + 1.1350L \cdot t_s \cdot N_b \quad (12)$$

Table 19. Percent Change in Rating Factors for Interior Moment for T-Beam Bridges

	d =	24				26				28				30			
	N_b =	3	4	5	6	3	4	5	6	3	4	5	6	3	4	5	6
L=34	S=6	-22	-6	19	63	-20	-4	19	56	-17	-3	18	50	-15	-1	17	44
	S=7	-18	1	31	89	-13	7	37	93	-7	13	44	98	0	21	51	103
	S=8	-14	8	46	124	-5	20	63	154	7	36	85	192	22	55	114	243
L=36	S=6	-22	-5	21	68	-21	-5	19	58	-19	-5	16	49	-17	-4	14	40
	S=7	-19	0	31	89	-15	4	34	89	-10	9	38	89	-5	14	42	88
	S=8	-17	5	41	116	-9	15	54	135	0	26	70	158	12	40	88	187
L=38	S=6	-22	-4	23	74	-21	-5	19	59	-21	-6	14	47	-20	-7	10	36
	S=7	-20	-1	30	90	-17	1	31	85	-14	4	32	80	-10	8	33	76
	S=8	-19	2	37	108	-13	9	46	119	-6	18	56	132	3	28	68	146
L=40	S=6	-22	-4	26	80	-22	-6	19	61	-22	-8	13	46	-22	-10	7	33
	S=7	-22	-2	29	90	-19	-1	28	81	-17	0	27	72	-14	2	26	64
	S=8	-21	-1	32	101	-16	4	38	105	-11	10	45	111	-4	17	52	116
L=42	S=6	-22	-3	28	87	-23	-6	19	63	-24	-9	11	44	-25	-12	4	29
	S=7	-23	-4	28	90	-21	-3	25	77	-20	-3	22	65	-18	-3	19	55
	S=8	-23	-4	28	94	-20	0	32	93	-15	4	35	93	-11	9	39	92

L = span length, in feet; S = girder spacing, in feet; d = beam depth, in inches; N_b = number of girders

Table 20. Percent Change in Distribution Factors for Exterior Moment for T-Beam Bridges

	t_s =	7			8			9		
	S =	6	7	8	6	7	8	6	7	8
L=34	N_b=3	-130	-101	-72	-29	-52	-75	71	-4	-79
	N_b=4	-71	-9	53	-8	2	12	54	13	-29
	N_b=5	-12	83	177	13	56	99	38	29	20
	N_b=6	47	174	302	34	110	186	22	46	70
L=36	N_b=3	-106	-82	-59	-15	-37	-59	76	8	-59
	N_b=4	-57	-6	45	-2	4	9	54	14	-26
	N_b=5	-8	70	148	12	45	77	32	19	7
	N_b=6	40	146	251	25	85	145	10	25	40
L=38	N_b=3	-82	-64	-46	-1	-22	-43	81	21	-39
	N_b=4	-43	-4	36	5	6	7	54	15	-23
	N_b=5	-5	57	119	11	33	56	26	10	-7
	N_b=6	34	117	201	16	61	105	-1	4	9
L=40	N_b=3	-58	-45	-33	14	-6	-26	86	33	-20
	N_b=4	-30	-1	28	12	8	4	53	16	-20
	N_b=5	-1	44	89	9	22	34	20	0	-21
	N_b=6	27	89	150	7	36	64	-13	-17	-21
L=42	N_b=3	-34	-27	-20	28	9	-10	91	45	0
	N_b=4	-16	2	20	18	10	1	53	18	-17
	N_b=5	2	31	60	8	10	13	14	-10	-34
	N_b=6	21	60	100	-2	11	24	-24	-38	-51

L = span length, in feet; S = girder spacing, in feet; N_b = number of girders; t_s = slab thickness, in inches

Table 21. Percent Change in Rating Factors for Exterior Moment for T-Beam Bridges

	t_s =	7			8			9		
	S =	6	7	8	6	7	8	6	7	8
L=34	N_b=3	-438	-13414	256	42	110	305	-41	4	370
	N_b=4	243	10	-35	9	-2	-11	-35	-11	41
	N_b=5	14	-45	-64	-12	-36	-50	-28	-23	-17
	N_b=6	-32	-64	-75	-26	-52	-65	-18	-32	-41
L=36	N_b=3	-1827	466	143	18	59	144	-43	-8	144
	N_b=4	133	7	-31	2	-4	-8	-35	-12	35
	N_b=5	9	-41	-60	-11	-31	-44	-24	-16	-6
	N_b=6	-29	-59	-72	-20	-46	-59	-9	-20	-28
L=38	N_b=3	454	177	85	1	28	74	-45	-17	65
	N_b=4	77	4	-27	-5	-5	-6	-35	-13	30
	N_b=5	5	-36	-54	-10	-25	-36	-21	-9	8
	N_b=6	-25	-54	-67	-14	-38	-51	1	-4	-8
L=40	N_b=3	139	83	49	-12	7	36	-46	-25	25
	N_b=4	42	1	-22	-10	-7	-4	-35	-14	25
	N_b=5	1	-31	-47	-9	-18	-25	-17	0	26
	N_b=6	-21	-47	-60	-7	-26	-39	15	20	27
L=42	N_b=3	52	37	25	-22	-8	11	-48	-31	0
	N_b=4	19	-2	-17	-15	-9	-1	-34	-15	21
	N_b=5	-2	-24	-37	-8	-9	-11	-12	11	52
	N_b=6	-17	-38	-50	2	-10	-19	32	61	106

L = span length, in feet; S = girder spacing, in feet; N_b = number of girders; t_s = slab thickness, in inches

Observations from these results include:

- As the slab thickness increased, the distribution factors tended to have a smaller reduction.
- For bridges with a slab thickness of 7 or 8 inches, as the number of girders increased, the potential reduction in distribution factor decreased. On the other hand, for bridges with a slab thickness of 9 inches, an increase in the number of girders mostly resulted in a higher possibility of reduction in distribution factors.
- For bridges with a slab thickness of 7 inches, increasing the girder spacing decreased the possibility of reduction in distribution factor. On the other hand, for bridges with a slab thickness of 8 or 9 inches, increasing girder spacing lead to higher reductions in the distribution factor.

Interior Shear. The regression model developed for interior shear is shown in Equation (13). This four-parameter model had an R^2 value of 0.7835 (78.35%). The primary parameters associated with this model are girder spacing, span length, skew angle, and number of girders. Tables 22 and 23 illustrate the impacts across the parameter space for both distribution factor and load rating factor.

$$\begin{aligned}\Delta DF_{int\text{-}S} = {} & -2343 + 68.18L + 281.1S + 22.78\theta + 457.7N_b - 8.14L \cdot S + 3.686L \cdot \theta \\ & -12.9L \cdot N_b - 19.33S \cdot \theta - 5635S \cdot N_b - 14.51\theta \cdot N_b - 102.1\times10^{3}L \cdot S \cdot \theta \\ & + 15600L \cdot S \cdot N_b - 0.749L \cdot \theta \cdot N_b + 6.119S \cdot \theta \cdot N_b\end{aligned} \quad (13)$$

Table 22. Percent Change in Distribution Factors for Interior Shear for T-Beam Bridges

	N_b =	3			4			5			6		
	S =	6	7	8	6	7	8	6	7	8	6	7	8
θ=0	L=34	18	24	30	16	22	28	14	20	25	12	17	22
	L=36	17	22	28	15	20	25	13	18	23	11	15	20
	L=38	15	20	26	13	18	23	11	16	20	9	13	18
	L=40	13	18	23	11	16	21	9	14	18	7	12	16
	L=42	12	16	21	10	14	18	8	12	16	6	10	13
θ=15	L=34	28	36	43	25	23	21	21	10	-1	18	-2	-23
	L=36	22	30	37	24	21	19	25	13	2	26	5	-15
	L=38	17	24	31	22	20	18	28	16	5	33	13	-8
	L=40	11	17	24	21	18	16	31	19	7	41	20	-1
	L=42	5	11	18	19	17	14	34	22	10	49	27	6
θ=30	L=34	38	47	56	33	24	15	29	1	-26	24	-22	-68
	L=36	28	37	46	32	23	14	37	9	-19	41	-5	-51
	L=38	18	27	36	31	22	12	44	17	-11	58	12	-34
	L=40	8	17	25	30	21	11	52	25	-3	75	28	-18
	L=42	-2	6	15	29	19	10	60	32	4	92	45	-1
θ=45	L=34	48	59	69	42	25	9	36	-8	-52	29	-42	-113
	L=36	34	44	55	41	24	8	48	5	-39	56	-15	-86
	L=38	20	30	41	40	24	7	61	17	-27	82	11	-60
	L=40	5	16	26	40	23	6	74	30	-14	108	37	-34
	L=42	-9	2	12	39	22	5	87	43	-2	134	63	-8

L = span length, in feet; S = girder spacing, in feet; N_b = number of girders; θ = skew in the bridge, in degrees

Table 23. Percent Change in Rating Factors for Interior Shear for T-Beam Bridges

	N_b =	3			4			5			6		
	S =	6	7	8	6	7	8	6	7	8	6	7	8
θ=0	L=34	-16	-20	-23	-14	-18	-22	-13	-16	-20	-11	-15	-18
	L=36	-14	-18	-22	-13	-17	-20	-11	-15	-18	-10	-13	-17
	L=38	-13	-17	-20	-12	-15	-19	-10	-14	-17	-8	-12	-15
	L=40	-12	-15	-19	-10	-14	-17	-9	-12	-15	-7	-10	-13
	L=42	-10	-14	-17	-9	-12	-16	-7	-11	-14	-5	-9	-12
θ=15	L=34	-22	-26	-30	-20	-19	-18	-18	-9	1	-15	2	29
	L=36	-18	-23	-27	-19	-18	-16	-20	-12	-2	-20	-5	18
	L=38	-14	-19	-23	-18	-17	-15	-22	-14	-4	-25	-11	9
	L=40	-10	-15	-20	-17	-15	-14	-24	-16	-7	-29	-17	1
	L=42	-5	-10	-15	-16	-14	-12	-25	-18	-9	-33	-22	-6
θ=30	L=34	-28	-32	-36	-25	-19	-13	-22	-1	36	-19	28	209
	L=36	-22	-27	-31	-24	-19	-12	-27	-8	23	-29	5	104
	L=38	-15	-21	-26	-24	-18	-11	-31	-14	12	-37	-10	52
	L=40	-7	-14	-20	-23	-17	-10	-34	-20	3	-43	-22	21
	L=42	2	-6	-13	-23	-16	-9	-38	-24	-4	-48	-31	1
θ=45	L=34	-32	-37	-41	-29	-20	-8	-26	9	108	-23	71	-895
	L=36	-25	-31	-35	-29	-20	-7	-33	-4	65	-36	18	641
	L=38	-16	-23	-29	-29	-19	-7	-38	-15	36	-45	-10	153
	L=40	-5	-14	-21	-28	-19	-6	-43	-23	16	-52	-27	52
	L=42	10	-2	-11	-28	-18	-5	-46	-30	2	-57	-39	9

L = span length, in feet; S = girder spacing, in feet; N_b = number of girders; θ = *skew in the bridge, in degrees*

Observations from these results include:

- Distribution factors mostly increased for bridges with characteristics that were within the bounds presented in Table 22.
- Increasing numbers of girders mostly leads to an increase in distribution factor.
- Bridges with a high skew angle (30 or 45 degrees) and high girder spacing may have a reduction in the distribution factor. The magnitude of this reduction increases with a decrease in span length.

Exterior Shear. The regression model developed for exterior shear is shown in Equation (14)**Error! Reference source not found.**. This four-parameter model had an R^2 value of 0.8941 (89.41%). The primary parameters associated with this model were moment of inertia, slab thickness, span length, and skew angle. Tables 24 and 25 illustrate the impacts across the parameter space for both distribution factor and load rating factor. Observations from these results include:

- Distribution factors mostly increased for bridges with characteristics that were within the bounds provided in Table 24.
- As the skew angle increased, the percent increase in distribution factor mostly increased.
- As the moment of inertia increased, the distribution factors tended to have a higher probability of an increase.

$$\begin{aligned}\Delta DF_{ext\text{-}S} = {} & -580.9 + 17.08L + 73.81t_s - 2.16L \cdot t_s - 16.76\times10^{-5}L \cdot I + 28.06\times10^{-2}L \cdot \theta \\ & -77.74\times10^{-2}t_s \cdot \theta + 2.216\times10^{-5}L \cdot t_s \cdot I - 1631\times10^{3}L \cdot t_s \cdot \theta \\ & -736.9\times10^{8}L \cdot I \cdot \theta + 4.026\times10^{-5}t_s \cdot I \cdot \theta\end{aligned} \quad (14)$$

Table 24. Percent Change in Distribution Factors for Exterior Shear for T-Beam Bridges

	t_s =	7				8				9			
	θ =	0	15	30	45	0	15	30	45	0	15	30	45
	L=34	-5	6	17	28	8	9	10	12	21	13	4	-4
	L=36	-1	7	15	23	9	9	9	9	18	10	2	-6
I=18000	**L=38**	3	8	14	19	9	8	7	5	15	7	0	-8
	L=40	7	10	12	15	10	7	5	2	12	5	-3	-10
	L=42	11	11	11	11	10	6	3	-1	9	2	-5	-12
	L=34	-9	12	32	52	8	18	29	39	25	25	26	26
	L=36	-5	12	28	44	9	17	25	33	23	23	22	22
I=24000	**L=38**	-1	12	24	36	10	16	21	27	21	20	19	17
	L=40	3	11	20	28	11	14	17	21	19	17	15	13
	L=42	7	11	16	20	12	13	14	14	17	14	11	8
	L=34	-12	17	47	77	8	28	47	67	28	38	48	57
	L=36	-8	16	41	65	9	26	42	58	27	35	42	50
I=30000	**L=38**	-5	15	34	53	11	23	36	48	26	32	37	43
	L=40	-1	13	28	42	12	21	30	39	26	29	32	36
	L=42	3	12	21	30	14	19	24	29	25	26	27	29

L = span length, in feet; S = girder spacing, in feet; I = girder moment of inertia, in inches^4; θ = skew in the bridge, in degrees

Table 252. Percent Change in Rating Factors for Exterior Shear for T-Beam Bridges

	t_s =	7				8				9			
	θ =	**0**	**15**	**30**	**45**	**0**	**15**	**30**	**45**	**0**	**15**	**30**	**45**
***I*=18000**	***L*=34**	6	-5	-14	-22	-7	-8	-9	-10	-18	-11	-4	4
	***L*=36**	1	-7	-13	-19	-8	-8	-8	-8	-15	-9	-2	7
	***L*=38**	-3	-8	-12	-16	-8	-7	-6	-5	-13	-7	0	9
	***L*=40**	-6	-9	-11	-13	-9	-7	-5	-2	-11	-5	3	11
	***L*=42**	-10	-10	-10	-10	-9	-6	-3	1	-8	-2	5	14
***I*=24000**	***L*=34**	10	-10	-24	-34	-7	-16	-22	-28	-20	-20	-21	-21
	***L*=36**	5	-10	-22	-31	-8	-15	-20	-25	-19	-18	-18	-18
	***L*=38**	1	-10	-19	-27	-9	-13	-18	-21	-17	-16	-16	-15
	***L*=40**	-3	-10	-17	-22	-10	-12	-15	-17	-16	-14	-13	-11
	***L*=42**	-6	-10	-14	-17	-11	-11	-12	-13	-14	-12	-10	-8
***I*=30000**	***L*=34**	14	-15	-32	-43	-7	-22	-32	-40	-22	-27	-32	-36
	***L*=36**	9	-14	-29	-39	-9	-20	-29	-37	-22	-26	-30	-33
	***L*=38**	5	-13	-25	-35	-10	-19	-26	-33	-21	-24	-27	-30
	***L*=40**	1	-12	-22	-29	-11	-17	-23	-28	-20	-22	-25	-26
	***L*=42**	-3	-11	-17	-23	-12	-16	-19	-23	-20	-21	-22	-22

L = span length, in feet; S = girder spacing, in feet; I = girder moment of inertia, in inches^4; θ = skew in the bridge, in degrees

Model Validation. The regression models were validated through a comparison of the predictions to the results directly derived from the refined analyses of the selected set of bridges. The change in the distribution factor for the moment and shear obtained from the refined analysis (x-axis) versus the regression model (y-axis) for each T-beam bridge are shown in Figure 16**Figure**. The solid line in the plots indicates no difference between these two calculations. The dashed lines in the plots represent the limits of 10% error between the regression model and the refined analysis model. The results indicated that the prediction model developed herein can make a reasonable estimate for the majority of the T-beam bridges used in this study for all load effect cases. Similar to the steel girder bridge predictions, as the bridges approached or extended beyond the parameter space, the models tended to lose accuracy, albeit with less extreme differences than the steel girder bridges.

Slab Bridges

Recall that the load rating factor for a slab structure is directly proportional to the effective width. The regression model developed for the slab bridge effective width is shown in Equation (15). This four-parameter model had an R^2 value of 0.9052 (90.52%). The primary parameters associated with this model were span length, bridge width, skew angle, and parapet width. Table 26 illustrates the impacts across the parameter space for effective width.

$$\Delta E_w = -289.4 + 23.09L + 10.07W + 57.88P_w + 10.73\theta - 8.102\times10^{-1}L \cdot W \quad (15)$$

$$-14.94L \cdot P_w - 52.89L \times 10^{-2} L \cdot \theta - 78.40 \times 10^{-2} W \cdot P_w - 30.06 \times 10^{-2} W \cdot \theta$$
$$+ 41.26 \times 10^{-2} P_w \cdot \theta + 49.21 \times 10^{-2} L \cdot W \cdot P_w + 14.71 \times 10^{-3} L \cdot W \cdot \theta$$
$$+ 13.97 \times 10^{-2} L \cdot P_w \cdot \theta - 11.93 \times 10^{-2} W \cdot P_w \cdot \theta$$

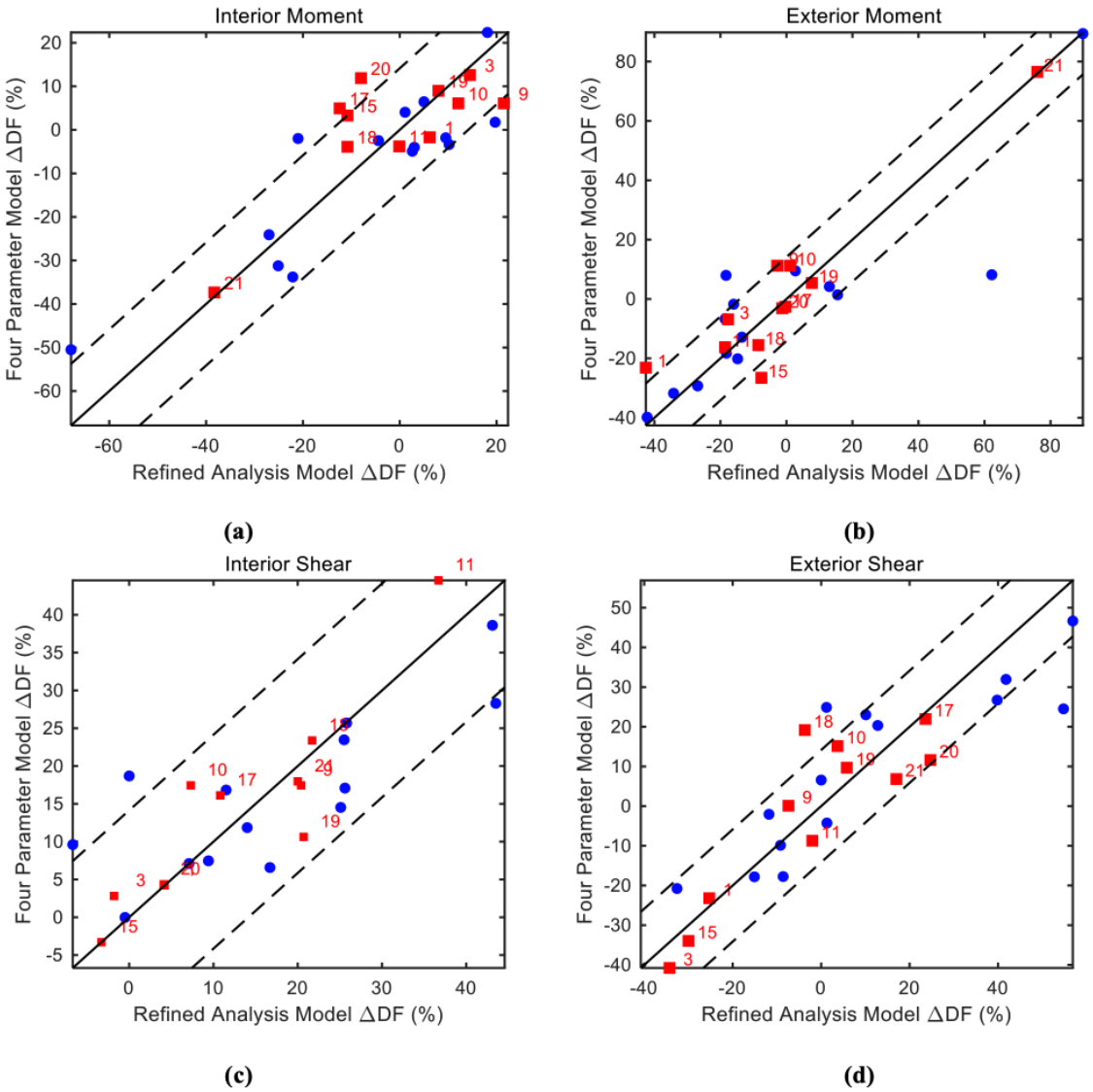

Figure 16. Percent Change in Distribution Factors for Reinforced Concrete T-Beam Bridges - Refined Analysis Versus Regression Model: (a) interior moment; (b) exterior moment; (c) interior shear; (d) exterior shear. Blue markers represent bridges within the parameter ranges of the regression model, while red markers represent bridges outside that range together with corresponding bridge numbers in Table 5.

Observations from these results include:

- Effective width mostly increased for bridges with characteristics that were within the defined bounds.
- Bridges with small span lengths mostly had a higher possibility of an increase in effective width.

- An increase in bridge width mostly lead to an increase in effective width.
- Bridges with larger parapet widths had a higher probability of an increase in effective width.

Table 26. Percent Change in Effective Width for Slab Bridges

	P_w =	1			1.12			1.25		
	W =	25	30	35	25	30	35	25	30	35
L=15	θ=0	4	26	49	3	30	57	3	34	65
	θ=15	8	16	24	7	18	28	6	20	34
	θ=30	13	6	-1	11	6	0	9	6	2
	θ=45	18	-4	-26	15	-6	-28	12	-8	-29
L=20	θ=0	5	19	34	3	23	43	1	27	53
	θ=15	8	13	18	6	16	26	5	19	34
	θ=30	11	7	3	10	9	8	9	12	14
	θ=45	14	1	-13	14	2	-9	13	4	-5
L=25	θ=0	6	12	19	2	16	29	-1	20	41
	θ=15	7	10	13	6	14	23	4	19	34
	θ=30	9	8	7	9	12	16	9	18	26
	θ=45	10	5	0	12	11	9	14	17	19
L=30	θ=0	7	5	4	2	9	16	-4	13	29
	θ=15	7	7	7	5	12	20	2	18	34
	θ=30	7	9	10	8	16	24	9	23	38
	θ=45	7	10	14	10	19	28	15	29	43

L = span length, in feet; W = slab width, in feet; P_w = parapet width, in feet; θ = skew in the bridge, in degrees

Model Validation. The predictions models developed were validated through a comparison of the effective width results derived from the direct refined analyses. The change in the effective width obtained from the refined analysis (x-axis) versus the regression model (y-axis) for each slab bridge are shown in Figure 17. The solid line in the plot indicate no difference

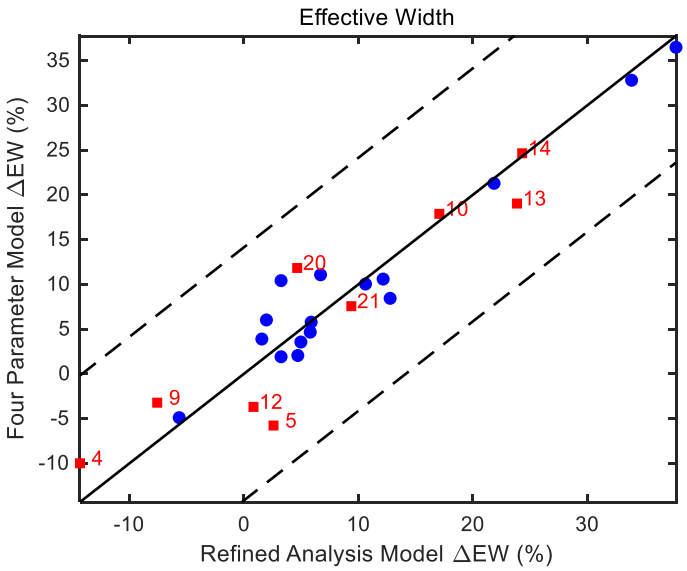

Figure 17. Percent Change in Effective Width for Reinforced Concrete Slab Bridges - Refined Analysis Versus Regression Model. Blue markers represent bridges within the regression model parameter ranges, while red markers are for bridges outside that range together with corresponding bridge numbers in Table 6.

between these two parameters. The dashed lines represent the limits of 10% error between the regression model and the refined analysis model. Note that in Table 26, the regression model estimates for the percent change in the effective width are provided for the bridges with span lengths of 25 ft, 30 ft, and 35 ft. In the results presented in Figure 17, there were a number of bridges with a span length greater than 40 ft or less than 15 ft, i.e. outside the model boundaries. Nevertheless, the regression model was able to make very close predictions for both bridges within and outside of the model boundaries. In particular, the mean deviation between the regression model estimate and refined analysis results for the change in the effective width was 2%.

CONCLUSIONS

- *The bridges in the VDOT inventory that are susceptible to load posting due to SHVs and EVs primarily consist of steel girder-concrete deck, reinforced concrete T-beam, and slab bridges.* There are a large number of steel girder bridges with timber deck that are rated below one for the SHVs; however, almost all of these bridges are located on secondary routes.

- *The plate with eccentric beam analysis (for girder bridges) and plate analysis (for slab bridges) are more effective refined analysis methods in representing the load distribution behavior when modeling with LARSA 4D.* For the eccentric beam analysis, LARSA 4D allows generating models automatically with little effort by using built-in templates that can also be modified using spreadsheets. While the basic grid analysis approach can work for both of these types of structures, using this method in LARSA 4D requires additional effort in placing grid lines and calculating some sectional properties.

- *The moment distribution factors obtained from the refined analysis will likely result in improved rating factors compared to those using distribution factors computed through the AASHTO LRFD approach, as is the case for the shear distribution factors for exterior girders.*

- *The shear distribution factors for interior girders determined through refined analysis will likely be greater than those calculated using the AASHTO LRFD approach.* Consequently, the rating factors for those bridges controlled by the shear capacity of interior beams will likely be lower.

- *For the slab bridges, refined analysis tends to result in a higher effective slab width when compared to the AASHTO LRFD approach.* Single-lane loading conditions will likely have a greater increase compared to multi-lane loaded cases.

RECOMMENDATIONS

1. *VDOT's Structure and Bridge Division should use the tables developed in this report as an initial screening tool to identify bridge structures within their inventory that are vulnerable to posting but have high potential for improvement in rating factors through the use of refined analyses.*

2. *VDOT's Structure and Bridge Division should employ a plate with eccentric beam approach to model girder bridges and 2D plate analysis approach for slab bridges when conducting refined analysis using LARSA 4D.*

IMPLEMENTATION AND BENEFITS

Implementation

In regards to recommendation 1, VDOT's Structure and Bridge Division will include the tables developed within this report in the scope of the Load Rating Manual as a means for VDOT's load rating engineers to quickly identify potential candidate bridges that would benefit from an improved load rating factor through refined analysis methods. The Load Rating Manual is currently scheduled to be finished by September 30, 2021.

In regards to recommendation 2, VDOT's Structure and Bridge Division will also include in the scope of the Load Rating Manual a recommendation for the load rating engineer to use the plate with eccentric beam analysis for girder bridges and plate analysis for slab bridges when using refined analysis methods for the purposes of establishing more precise load distribution behavior in its girder-concrete deck and slab bridges. The Load Rating Manual is currently scheduled to be finished by September 30, 2021.

Benefits

With regards to recommendations 1 and 2, VDOT can continue to be in compliance with federal mandates regarding the new SHV and EV load rating classifications. Beyond that, however, many other bridges are on the cusp of posting requirements for the more traditional load rating vehicles. At a time when VDOT must prioritize spending decisions for maintenance, rehabilitation, and reconstruction, the tools generated from this research can help to alleviate the pressure by offering more precision on the rating factors, resulting in a greater number of bridges with a sufficient level of safety. This result will mitigate the number of unnecessarily posted structures due to conservative calculations, and thus help to maintain the level of travel and commerce across the Commonwealth.

ACKNOWLEDGEMENTS

The research team would like to acknowledge the support provided by VDOT in execution of this research. This acknowledgement includes the TRP for providing guidance on the project direction as well as the various districts.

REFERENCES

Adams, A., Galindez, N., Hopper, T., Murphy, T., Ritchie, P., Storlie, V., and Weisman, J. (2019). *Manual for Refined Analysis in Bridge Design and Evaluation* (No. FHWA-HIF-18-046). United States. Federal Highway Administration. Office of Infrastructure.

Amer, A., Arockiasamy, M. and Shahawy, M. (1999). Load distribution of existing solid slab bridges based on field tests. *Journal of Bridge Engineering*, 4(3), pp.189-193.

American Association of State and Highway Transportation Officials (AASHTO) (2019). *Manual for Bridge Evaluation*. 3rd Ed. with 2019 Interim Revisions. American Association of State Highway and Transportation Officials, Washington, DC.

American Association of State Highway and Transportation Officials (AASHTO) (2017). *AASHTO LRFD Bridge Design Specifications*. 8th Ed. American Association of State Highway and Transportation Officials, Washington, DC.

Barker, M.G. (2001). Quantifying field-test behavior for rating steel girder bridges. *Journal of Bridge Engineering*, 6(4), pp.254-261.

Catbas, F.N., Gokce, H.B. and Gul, M. (2012). Practical approach for estimating distribution factor for load rating: Demonstration on reinforced concrete T-beam bridges. *Journal of Bridge Engineering*, 17(4), pp.652-661.

Chiewanichakorn, M., Aref, A.J., Chen, S.S. and Ahn, I.S. (2004). Effective flange width definition for steel–concrete composite bridge girder. *Journal of Structural Engineering*, 130(12), pp.2016-2031.

Chung, W., Liu, J. and Sotelino, E.D. (2006). Influence of secondary elements and deck cracking on the lateral load distribution of steel girder bridges. *Journal of Bridge Engineering*, 11(2), pp.178-187.

Davids, W.G., Poulin, T.J. and Goslin, K. (2013). Finite-element analysis and load rating of flat slab concrete bridges. *Journal of Bridge Engineering*, 18(10), pp.946-956.

Dymond, B.Z., French, C.E. and Shield, C.K. (2019). Recommendations for More Accurate Shear Rating of Prestressed Concrete Girder Bridges. *Journal of Bridge Engineering*, 24(12), p.04019117.

Eom, J. and Nowak, A.S. (2001). Live load distribution for steel girder bridges. *Journal of Bridge Engineering*, 6(6), pp.489-497.

Federal Highway Administration (FHWA) (2013). *Action: Load Rating of Specialized Hauling Vehicles*. Federal Highway Administration, McLean, VA.

Federal Highway Administration (FHWA) (2016). *Fixing America's surface transportation act or 'FAST Act'*. Federal Highway Administration, McLean, VA.

Harris, D.K. (2010). Assessment of flexural lateral load distribution methodologies for stringer bridges. *Engineering Structures*, 32(11), pp.3443-3451.

Harris, D.K., Ozbulut, O., Bagheri, A., Dizaji, M.S., Ndong, A.K. and Alipour, M. (2020). *Load Rating Strategies for Bridges With Limited or Missing As-Built Information* (No. FHWA/VTRC 20-R27). University of Virginia.

Hawkins, D.M. and Galpin, J.S. (1986). Selecting a Subset of Regression Variables so as to Maximize the Prediction Accuracy at a Point. *Journal of Applied Statistics*, 13, pp.187-199.

Islam, S. (2018). *Load Rating Study of Effects of Special Hauling Vehicle Loads on Ohio Bridges* (Doctoral dissertation, University of Toledo).

Jáuregui, D.V., Licon-Lozano, A. and Kulkarni, K., 2007. *Improved load rating of reinforced concrete slab bridges* (No. NM05STR-02). New Mexico. Dept. of Transportation. Research Bureau.

Kim, S. and Nowak, A.S. (1997). Load distribution and impact factors for I-girder bridges. *Journal of Bridge Engineering*, 2(3), pp.97-104.

LARSA, Inc. LARSA, Melville, NY.

Mabsout, M., Tarhini, K., Jabakhanji, R. and Awwad, E. (2004). Wheel load distribution in simply supported concrete slab bridges. *Journal of Bridge Engineering*, 9(2), pp.147-155.

Mathworks, Inc. MATLAB, Natick, MA.

Nouri, G. and Ahmadi, Z. (2012). Influence of skew angle on continuous composite girder bridge. *Journal of Bridge Engineering*, 17(4), pp.617-623.

Nowak, A.S. and Eom, J. (2001). Verification of Girder Distribution Factors and Dynamic Load Factors by Field Testing. *Current and future trends in bridge design, construction and maintenance 2: Safety, economy, sustainability and aesthetics* (pp. 414-423). Thomas Telford Publishing.

R Core Team (2013). R: A language and environment for statistical computing. R Foundation for Statistical Computing, Vienna, Austria

Sivakumar, B. (2007). NCHRP 12-63: *Legal truck loads and AASHTO legal loads for posting*. Report 575, National Cooperative Highway Research Board, Washington, D.C.

Snyder, R. and Beisswenger, J. (2017). *Implementation of a Refined Shear Rating Methodology for Prestressed Concrete Girder Bridges* (No. MN/RC 2017-48). Minnesota. Dept. of Transportation. Research Services & Library.

Virginia Department of Transportation (VDOT) (2019). *State of the Structures and Bridges Report*. Virginia Department of Transportation, Richmond, VA.

Yousif, Z. and Hindi, R. (2007). AASHTO-LRFD live load distribution for beam-and-slab bridges: Limitations and applicability. *Journal of Bridge Engineering*, 12(6), pp.765-773.

Zokaie, T., Imbsen, R. A., and Osterkamp, T. A. (1991). *Distribution of Wheel Loads on Highway Bridges*, National Cooperative Highway Research Program (NCHRP 12-26). Transportation Research Board, Washington, USA.